โครงสร้างอิเล็กตรอนและโครงสร้างโมเลกุลที่สถานะพื้นของ Fe_2 Fe_2^+ Fe_2^{++} และ Fe_2^- คลัสเตอร์

นายวิวัฒน์ วชิรวงศ์กวิน

วิทยานิพนธ์นี้เป็นส่วนหนึ่งของการศึกษาตามหลักสูตรปริญญาวิทยาศาสตรมหาบัณฑิต

สาขาวิชาเคมี ภาควิชาเคมี

คณะวิทยาศาสตร์ จุฬาลงกรณ์มหาวิทยาลัย

ปีการศึกษา 2544

ISBN 974-03-0619-5

GROUND-STATE ELECTRONIC AND MOLECULAR STRUCTURES OF Fe_2, Fe_2^+, Fe_2^{++} AND Fe_2^- CLUSTERS

Mr. Viwat Vchirawongkwin

A Thesis Submitted in Partial Fulfillment of the Requirements
for the Degree of Master of Science in Chemistry
Department of Chemistry
Faculty of Science
Chulalongkorn University
Academic Year 2001
ISBN 974-03-0619-5

Thesis Title	GROUND-STATE ELECTRONIC AND MOLECULAR STRUCTURES OF Fe_2, Fe_2^+, Fe_2^{++} AND Fe_2^- CLUSTERS
By	Viwat Vchirawongkwin
Department	Chemistry
Thesis Advisor	Associate Professor Dr. Vudhichai Parasuk

Accepted by the Faculty of Science, Chulalongkorn University in Partial Fulfillment of the Requirements for the Master's Degree

.....Dean of Faculty of Science
(Associate Professor Wanchai Phothiphichitr, Ph.D.)

THESIS COMMITTEE

.....Chairman
(Associate Professor Sirirat Kokpol, Ph.D.)

.....Thesis Advisor
(Associate Professor Vudhichai Parasuk, Ph.D.)

.....Member
(Oravan Sanguanruang, Ph.D.)

.....Member
(Associate Professor Supot Hannongbua, Ph.D.)

.....Member
(Assistant Professor Warinthorn Chavasiri, Ph.D.)

วิวัฒน์ วชิรวงศ์กวิน : โครงสร้างอิเล็กตรอนและโครงสร้างโมเลกุลที่สถานะพื้นของ Fe_2 Fe_2^+ Fe_2^{++} และ Fe_2^- คลัสเตอร์ (GROUND-STATE ELECTRONIC AND MOLECULAR STRUCTURES OF Fe_2, Fe_2^+, Fe_2^{++} AND Fe_2^- CLUSTERS) อาจารย์ที่ปรึกษา: รศ.ดร. วุฒิชัย พาราสุข 73 หน้า. ISBN 974-03-0619-5

ได้ศึกษาโครงสร้างอิเล็กตรอนและโมเลกุลของ Fe_2 Fe_2^+ Fe_2^{++} และ Fe_2^- ด้วยวิธี มัลติคอนฟิกุเรชัน เซล์ฟคอนซิสเทนท์ฟิลด์ (MCSCF) และ มัลติเรฟเฟอเรนซ์ คอนฟิกุเรชันอินเทอแรกชัน (MRCI) กับเบซิสเซตหลายชนิด สำหรับ Fe_2 พบว่ามีสถานะพื้นเป็น $^7\Delta_u$ ด้วยโครงสร้างอิเล็กตรอน $\sigma^4\pi^6\delta^6$ ซึ่งเป็นโครงสร้างที่มีความแตกต่างอย่างชัดเจนกับผลการศึกษาที่ผ่านมา ผลการคำนวณให้ระยะระหว่างนิวเคลียส (R_e) 4.15 บอห์ร และ ความถี่มูลฐาน (ω_e) 215.0 cm^{-1} อันเป็นผลที่สอดคล้องอย่างดีกับผลการทดลอง R_e และ ω_e 3.53 $\pm$0.24 หรือ 3.82 $\pm$0.04 บอห์ร และ 299.6 cm^{-1} ตามลำดับ สำหรับ Fe_2^+ พบว่ามีสถานะพื้นเป็น $^8\Delta_u$ ซึ่งมี R_e และ ω_e 4.49 บอห์ร และ 159.6 cm^{-1} ตามลำดับ สำหรับ Fe_2^- มีสถานะพื้นเป็น $^8\Delta_g$ ซึ่งมี R_e และ ω_e 4.03 (3.89-4.04) บอห์ร และ 278.2 (250$\pm$20) cm^{-1} ตามลำดับ (ค่าจากการทดลองแสดงในวงเล็บ) สำหรับ Fe_2^{++} ระหว่าง 4 สถานะที่ศึกษาพบว่า $^9\Pi_g$ เป็นสถานะพื้นซึ่งมีพลังงานต่ำกว่าสถานะข้างเคียงประมาณ 30 kcal/mol R_e และ ω_e ของสถานะนี้มีค่า 5.16 บอห์ร และ 176.5 cm^{-1} ตามลำดับ ในการศึกษานี้ค่าพลังงานการเกิดไอออนอันดับที่ 1 และ 2 ของ Fe_2 ที่คำนวณได้ มีค่าเท่ากับ 5.1 และ 15.9 eV ตามลำดับ ในขณะที่ค่าพลังงานการเกิดไอออนอันดับที่ 1 จากผลการทดลองมีค่า 6.30$\pm$0.01 eV ส่วนค่าสัมพันธภาคอิเล็กตรอนที่คำนวณได้ 0.316 eV นั้นมีค่าต่ำเกินไปเมื่อเปรียบเทียบกับผลจากการทดลองซึ่งมีค่าเท่ากับ 0.902 $\pm$ 0.008 eV การคำนวณยังแสดงให้เห็นว่า Fe_2 สามารถรับอิเล็กตรอนได้ง่ายกว่าที่จะสูญเสียอิเล็กตรอน

ภาควิชา....เคมี..... ลายมือชื่อนิสิต.....

สาขาวิชา....เคมีวิเคราะห์..... ลายมือชื่ออาจารย์ที่ปรึกษา.....

ปีการศึกษา..2544..... ลายมือชื่ออาจารย์ที่ปรึกษาร่วม.....

VIWAT VCHIRAWONGKWIN: GROUND-STATE ELECTRONIC AND MOLECULAR STRUCTURES OF Fe_2, Fe_2^+, Fe_2^{++} AND Fe_2^- CLUSTERS. THESIS ADVISOR: ASSOC. PROF. VUDHICHAI PARASUK, Ph.D. 73 pp. ISBN 974-03-0619-5

The electronic and the molecular structures of Fe_2, Fe_2^+, Fe_2^{++}, and Fe_2^- were investigated using the multiconfiguration self consistent-field (MCSCF) and multireference configuration interaction (MRCI) methods with various basis sets. For Fe_2, the ground state is the $^7\Delta_u$ with $\sigma^4\pi^6\delta^6$ electronic structure, the structure which is markedly different from the previous studies. The equilibrium nuclear distance (R_e) of 4.15 Bohr and the zero-point frequency (ω_e) of 215.0 cm^{-1} were obtained. This is in good agreement with the experimental R_e and ω_e of 3.53±0.24 or 3.82±0.04 Bohr and 299.6 cm^{-1}, respectively. For Fe_2^+, the ground state is the $^8\Delta_u$ with R_e and ω_e of 4.49 Bohr and 159.6 cm^{-1}, respectively. For Fe_2^-, the ground state is $^8\Delta_g$ state with R_e and ω_e of 4.03 (3.89-4.04) Bohr and 278.2 (250±20) cm^{-1}, respectively (the experimental values are given in parentheses). For Fe_2^{++}, among 4 states investigated the $^9\Pi_g$ is the ground state with the energy around 30 kcal/mol below the next lowest state. The R_e and ω_e for this state are 5.16 Bohr and 176.5 cm^{-1}, respectively. In this study, the first and the second ionizations of Fe_2 are 5.1 and 15.9 eV, respectively while the experimental value is 6.30±0.01 eV. The calculated electron affinity of 0.316 eV is underestimated in comparison with the experimental value of 0.902±0.008 eV. The calculations also showed that it is easier for Fe_2 to accept than to lose electron.

Department ...Chemistry..... Student's signature .....

Field of study ...Physical Chemistry... Advisor's signature ...Vudhichai Parasuk...

Academic year ...2001..... Co-advisor's signature .....

ACKNOWLEDGEMENT

First of all, the author wishes to express his deepest appreciation to his advisor, Associate Professor Vudhichai Parasuk, Ph.D., for encouring guidance, supervision and beneficial suggestions throughout the course of this research.

Greatful acknowledgements are made to Associate Professor Sirirat Kokpol, Ph.D., Oravan Sanguanruang, Ph.D., Associate Professor Supot Hannongbua, Ph.D., and Assistant Professor Warinthorn Chavasiri, Ph.D. for serving as Examination Commitee Members.

Thanks also for Professor Keiji Morokuma of the Emory University, U.S.A. for his insightful suggestions on the calculations of Fe_2.

The author also whishes to extend his profound thanks to his friend for their cooperation and mental supports during this work.

Last but not least the author would like to dedicate this master thesis with great respect and love to his family for all things that they have endured and sacrificed for his success.

CONTENTS

LIST OF TABLES

LIST OF FIGURES

CHAPTER I

INTRODUCTION

Recently there exists the nano-scale synthetic of transition metal clusters which forms charged dielectric nanospheres called quantum drop. Interestingly, the physcial and chemical properties of these clusters differ somewhat from their bulk. It was found that both neutral and ionic forms of the metal clusters involve in catalysis processes. For example, the clusters of iron were observed during the catalysis progress [1] and, hence, its properties have been of interest. Since, the electron configuration of the iron atom is d^6 which enables to form many oxidation states. Thus, the electron configuration of iron cluster is very complex. Among the iron clusters, the iron dimer, Fe_2, has been subjected to the most number of studies. Its electronic ground state configuration was proposed by many people (see Table **1**). [5, 6, 7, 8, 9] Although it is now well accepted that the ground state of Fe_2 is $^7\Delta_u$ state, the electronic configuration of this state is still far from reaching the conclusion.

1.1 Previous studies on Fe_2 cluster

In 1980, P.A. Montano and G.K. Shenoy reported the internuclear distance of Fe_2 from the extended X-ray absorption fine structure (EXAFS) experiment in argon matrix to be 1.87 ± 0.13 Å. [2] Later in 1982, H. Purdum and co-workers obtained the Fe-Fe distance of 2.02 ± 0.02 Å using EXAFS but performed in neon

matrix. [3] The later work is considered to be more accurate and the accepted distance is 2.00 - 2.04 Å or 3.78 - 3.86 Bohr. Several experiments were also carried out to elucidate other properties of Fe_2. In 1984, E.A. Rohlfing and co-workers using laser photoionization spectra obtained the first ionization potential of 6.30 ± 0.01 eV for Fe_2. [1] In 1986, D.G. Leopold and W.C. Lineberger using photoelectron spectra investigated the anion Fe_2^- and the values of 0.902 ± 0.008 eV for the electron affinity of the Fe_2 was reported together with, for the bond elongation of 2.10 ± 0.04 Å, and the zero-point frequency (ω_e) of 250 ± 20 cm^{-1}. [4] Since there is very much limitation on the experimental side to determine the electronic structure of Fe_2, several theoretical studies were launched. The comparison of these studies were shown in Table **1**. In 1979, J. Harris and R.O. Jones carried out calculations using density functional theory (DFT) and found the $^7\Delta_u$ as the ground state with $1\sigma_g^2\ 2\sigma_g^2\ \pi_u^4\ \delta_g^3\ \delta_u^2\ \pi_g^2\ 1\sigma_u^1$ electronic configuration with the equilibrium nuclear distance of 3.96 Bohr (2.09 Å) and zero-point frequency of 390 cm^{-1}. [5] In 1981, D. Guenzburger and E.M.B. Saitovitch using SCF-X_α-SW (an DFT method) calculated isomer shift (IS) as well as quadrupole splitting (QS). They found that when using the configuration of ($6\sigma_g^2\ 6\sigma_u^1\ 3\pi_u^4\ 3\pi_g^3\ 1\delta_g^2\ 1\delta_u^2\ 4s\sigma_g^2$) which corresponds to $^7\Pi_u$ state the results were very agreeable to the experiments. [6] In 1982, I. Shim and K.A. Gingerich using *ab initio* Hartree-Fock (HF) and configuration interaction (CI), with double zeta quality basis and the triple zeta function for *3d* orbital again obtained the $^7\Delta_u$ state for the ground state and the configuration $3d\sigma_g^{1.57}\ 3d\pi_u^{3.06}\ 3d\delta_g^{2.53}\ 3d\delta_u^{2.47}\ 3d\pi_g^{2.89}\ 3d\sigma_u^{1.49}\ 3d\sigma_g^{2.00}$ was given. Though both Harris and Jones and Shim and Gingerich reported the same state as the groundstate, however, the reported electron configurations are markedly different. Furthermore, the equilibrium nuclear distance of 4.54 Bohr (2.40 Å), and zero-point frequency of 204 cm^{-1} were obtained. [7] This however

emphasizes the weakness of Shim and Gingerich's result. In 1988, M. Tomonari and H. Tatewaki performed *ab initio* SCF and CI calculation and the $^7\Delta_u$ state were suggested the ground state of Fe_2 molecule with the equilibrium nuclear distance of 2.02 Å. Amazingly, this bond distance is within the error of the experiments. They, furthermore, gave the configuration of ($6\sigma_g^{1.9}$ $6\sigma_u^{1.1}$ $3\pi_g^{2.3}$ $3\pi_u^{3.7}$ $1\delta_g^{2.8}$ $1\delta_u^{2.2}$ $4s\sigma_g^{2.0}$) for the ground state. Moreover, they also calculated the anionic state where the $^8\Delta_g$ state with R_e and ω_e of 2.05 Å and 370 cm^{-1}, respectively was yielded. From the result, they computed the electron affinity and the value of 0.45 eV was obtained. [8]

Interestingly, there is quite a disagreement between two CI calculations (Shim-Gingerich and Tomonari-Tatewaki) in the electron configuration of Fe_2. For the moment, the most trusted theoretical result is that of Tomonari and Tatewaki's. Still their electron affinity is overly underestimated. From the complexity of the electronic structure of Fe_2, the near-degeneracy correlation which is lacked in previous studies is supposed to be a crucial factor for determining the electronic structure of Fe_2 correctly. It is, therefore, our task to perform calculations that includes such a correlation to obtain the more accurate results.

Table 1: The electron configuration of Fe_2 dimer in the previous studies.

The electron configuration	Ground state	Ref.
$3d\sigma_g^{2.0}3d\pi_u^{4.0}3d\delta_g^{3.0}3d\delta_u^{2.0}3d\pi_g^{2.0}3d\sigma_u^{1.0}4s\sigma_g^{2.0}$	$^7\Delta_u$	Harris et al. [5]
$3d\sigma_g^{2.0}3d\pi_u^{4.0}3d\delta_g^{2.0}3d\delta_u^{2.0}3d\pi_g^{3.0}3d\sigma_u^{1.0}4s\sigma_g^{2.0}$	$^7\Pi_u$	Guenzburger et al. [6]
$3d\sigma_g^{1.6}3d\pi_u^{3.1}3d\delta_g^{2.5}3d\delta_u^{2.5}3d\pi_g^{2.9}3d\sigma_u^{1.5}4s\sigma_g^{2.0}$	$^7\Delta_u$	Shim et al. [7]
$3d\sigma_g^{1.9}3d\pi_u^{3.7}3d\delta_g^{2.8}3d\delta_u^{2.2}3d\pi_g^{2.3}3d\sigma_u^{1.1}4s\sigma_g^{2.0}$	$^7\Delta_u$	Tomonari et al. [8]
$3d\sigma_g^{2.0}3d\pi_u^{4.0}3d\delta_g^{2.0}3d\delta_u^{2.0}3d\pi_g^{2.0}3d\sigma_u^{2.0}4s\sigma_g^{2.0}$	$^7\Sigma_u$	Nagarathna et al. [9]

1.2 Scope of this Study

The systems under investigation in this study consisted of Fe_2, Fe_2^-, Fe_2^+ and Fe_2^{++} clusters. The *ab initio* Multiconfiguration Self-Consistent Field (MCSCF) and Multi-Reference Configuration Interaction (MRCI) calculations were carried out for such systems to elucidate their electronic stuctures and find their equilibrium nuclear distances (R_e) and the zero-point frequencies (ω_e). The first and second ionization energy were also computed from the energy difference between Fe_2 and Fe_2^+ and between Fe_2^+ and Fe_2^{++}, respectively. The electron affinity were computed from the energy difference between Fe_2 and Fe_2^-.

CHAPTER II

THEORETICAL METHODS

For tiny particles, Newtonian mechanics can not be applied. The quantum mechanics are then introduced, in which any properties can be calculated based on the solution of the time-independent Schrödinger equation

$$\hat{\mathrm{H}}\Psi = E\Psi. \tag{2.1}$$

Here, $\hat{H}$ stands for the Hamiltonian operator and E for the energy. In the system of n electrons and M nuclei, the nonrelativistic Hamiltonian in atomic unit is given by

$$\begin{aligned}\hat{\mathrm{H}} = &-\sum_{i=1}^{n}\frac{1}{2}\nabla_i^2 - \sum_{A=1}^{M}\frac{1}{2M_A}\nabla_A^2 - \sum_{i=1}^{n}\sum_{A=1}^{M}\frac{Z_A}{r_{iA}} \\ &+\sum_{i=1}^{n}\sum_{j>i}^{n}\frac{1}{r_{ij}} + \sum_{A=1}^{M}\sum_{B>A}^{M}\frac{Z_A Z_B}{R_{AB}}\end{aligned} \tag{2.2}$$

where ∇^2 is the Laplacian operator

$$\nabla^2 = \frac{\partial^2}{\partial x^2} + \frac{\partial^2}{\partial y^2} + \frac{\partial^2}{\partial z^2}, \tag{2.3}$$

From (2.2), M_A and Z_A are refered to mass and charge of the Ath nucleus respectively, R_{AB} stands for the distance between the Ath and B^{th} nucleus, while r_{ij} for the distance between the ith and j^{th} electron, and r_{iA} is the distance between the ith electron and the Ath nucleus. Unfortunately, the analytic solutions of the Schrödinger equation can be found only for a few simple one-electron systems such as the one-electron hydrogen atom and the H_2^+ molecule. Hence, the approximations must be introduced for the many-electron system. [10]

The first approximation to be applied is the Born-Oppenheimer approximation. In this approximation electron and nuclear motions are separated when the exact stationary states are applied to the nucleus. Therefore, Coulombic energy is obtained in a simple calculation. The application of the Born-Oppenheimer approximation reduced the once complicated problem to solving only the electronic part of the Schrödinger equation. Still the electronic part is too complex to be solved analytically. Further approximations must be introduced.

There are many approximations in quantum chemistry, for examples Hartree-Fock (HF) approximation, Multiconfiguration self-consistent field (MCSCF) theory, Configuration interaction (CI) theory, Coupled-cluster (CC) theory, Perturbation theory, Density-Functional theory and so on. In this thesis, the CI and the MCSCF methods were employed and only the theoretical background of these methods were discussed.

It is known that the HF theory is not sufficient to describe the many-electron system accurately. This is because, the method only contains the correlation of electrons with the same spin, the so called "Fermi correlation". However, the inclusion of the electron correlation of the electron with different spin, the so called "coulomb correlation", is also of importance and could not be neglected. In the electronic structure theory, the term *electron correlation* often refers to the correlation of the coulomb holes or the correction to the HF. The difference between the exact non-relativistic energy, E^{exact}, and the HF energy, E^{HF}, is called the correlation energy, E^{corr}.

$$E^{corr} = E^{exact} - E^{HF} \tag{2.4}$$

The contribution to the E^{corr} could be divided into the *near-degeneracy correlation*

or the *static correlation* and the *dynamic correlation*. The former arises when there exists many low-lying electronic states which are coupled to the ground state, or in the other words when one or more configurations are strongly coupled with the Hartree-Fock wave function. This correlation describes, for examples, the molecular bond dissociation, multiple weak bonds, transition metal compounds, *etc.* A correlated method that can account for this near-degeneracy correlation is the MCSCF. The latter is associated to the motions of electrons further from the nucleus. Usually, this correlation does not involve configurations which strongly mixed with the Hartree-Fock wave function. The dynamic correlation describes, for examples, the highly conjugated systems, the electric polarizability, *etc.* The dynamic correlation can be accounted for by several techniques including the CI.

2.1 Multiconfigurational Self-Consistent Field Theory

In the derivation of MCSCF equations [11, 12], it is convenient to define the wave function, the energy, and also the Hamiltonian in the second quantization formulae. In the 2nd quantization, 2 operators *i.e.* the creation, $a_i^\dagger$, and the annihilation, a_i operators were introduced. The properties of the creation and the annihilation operators are given by;

$$a_i^\dagger|\chi_k \cdots \chi_l\rangle = |\chi_i\chi_k \cdots \chi_l\rangle \quad \text{and} \quad a_i^\dagger|\chi_k \cdots \chi_l\rangle = 0 \quad \text{if} \quad i \in \{k, \ldots, l\} \tag{2.5}$$

$$a_i|\chi_i\chi_k \cdots \chi_l\rangle = |\chi_k \cdots \chi_l\rangle \quad \text{and} \quad a_i|\chi_k \cdots \chi_l\rangle = 0 \quad \text{if} \quad i \notin \{k, \ldots, l\}. \tag{2.6}$$

Anti-commutation relations of these operators are

$$\begin{aligned} a_i a_j + a_j a_i &= 0 \\ a_i^\dagger a_j^\dagger + a_j^\dagger a_i^\dagger &= 0 \\ a_i^\dagger a_j + a_j a_i^\dagger &= \delta_{ij}. \end{aligned} \tag{2.7}$$

The non-relativistic Hamiltonian in the second quantization formulism is

$$\hat{\mathbf{H}} = \sum_{i,j} h_{ij}\hat{E}_{ij} + \frac{1}{2}\sum_{i,j,k,l} g_{ijkl}(\hat{E}_{ij}\hat{E}_{kl} - \delta_{jk}\hat{E}_{il}). \tag{2.8}$$

The h_{ij} and g_{ijkl} are the one- and two-electron operators, respectively. The excitation operator $\hat{E}_{ij}$ is introduced as

$$\hat{E}_{ij} = \hat{a}^{\dagger}_{i\alpha}\hat{a}_{j\alpha} + \hat{a}^{\dagger}_{i\beta}\hat{a}_{j\beta}. \tag{2.9}$$

Matrix elements of one- and two-electron operators on Slater determinants $|m\rangle$ and $|n\rangle$ are

$$\langle m|\hat{H}_1|n\rangle = \sum_{i,j} h_{ij}\langle m|\hat{E}_{ij}|n\rangle = \sum_{i,j} h_{ij}D^{mn}_{ij} \tag{2.10}$$

and

$$\langle m|\hat{H}_2|n\rangle = \sum_{i,j,k,l} g_{ijkl}\langle m|\hat{E}_{ij}\hat{E}_{kl} - \delta_{jk}\hat{E}_{il}|n\rangle = \sum_{i,j,k,l} g_{ijkl}P^{mn}_{ijkl}. \tag{2.11}$$

The D^{mn}_{ij} and P^{mn}_{ijkl} are one- and two-electron coupling coefficients, respectively. Where

$$\begin{aligned} D^{mn}_{ij} &= \langle\Psi|\hat{E}_{ij}|\Psi\rangle \\ &\sum_{m,n} c^*_m c_n D^{mn}_{ij} \end{aligned} \tag{2.12}$$

is the element of the first order reduced density matrix and

$$P^{mn}_{ijkl} = \sum_{m,n} c^*_m c_n P^{mn}_{ijkl} \tag{2.13}$$

is the element of the second order reduced density matrix. Thus, the energy expression in the second quantization is

$$E = \langle\Psi|\hat{H}|\Psi\rangle = \sum_{i,j} h_{ij}D_{ij} + \sum_{i,j,k,l} g_{ijkl}P_{ijkl}. \tag{2.14}$$

The MCSCF energy is obtained by optimized both orbitals and MCSCF coefficients until the energy (2.14) is at minimum.

Consider the unitary transformation of orbitals

$$\phi' = \phi U \tag{2.15}$$

or

$$\hat{a}_i'^{\dagger} = \sum_k \hat{a}_k^{\dagger} U_{ki} \tag{2.16}$$

where

$$U^{\dagger} U = 1. \tag{2.17}$$

In the above equation U represents the unitary matrix. The unitary matrix U can be written as an exponential of the anti-Hermitian matrix T

$$U = e^{-T} \tag{2.18}$$

where

$$T = \sum_{i,j} T_{ij} a_i^{\dagger} a_j^{\dagger}. \tag{2.19}$$

The unitary matrix, U, in (2.15) can be expaned in Taylor's series

$$\begin{aligned} \hat{a}_i'^{\dagger} &= \hat{a}_i^{\dagger} - \sum_k \hat{a}_k^{\dagger} (\hat{T})_{ki} + \frac{1}{2} \sum_k \hat{a}_k^{\dagger} (\hat{T}^2) + \ldots \\ &= \sum_k \hat{a}_k^{\dagger} (e^{-\hat{T}})_{ki}. \end{aligned} \tag{2.20}$$

For the singlet system, the operator T is expressed by

$$\begin{aligned} \hat{T} &= \sum_{i,j} T_{ij} (\hat{a}_{i\alpha}^{\dagger} \hat{a}_{j\alpha} + \hat{a}_{i\beta}^{\dagger} \hat{a}_{j\beta}) \\ &= \sum_{i,j} T_{ij} \hat{E}_{ij}. \end{aligned} \tag{2.21}$$

In (2.21), when only the real part of T operator is considered we obtained

$$\begin{aligned}\hat{T} &= \sum_{i>j} T_{ij}(\hat{E}_{ij} - \hat{E}_{ji}) \\ &= \sum_{i>j} T_{ij}\hat{E}_{ij}^{-}\end{aligned} \tag{2.22}$$

where $\hat{E}_{ij}^{-}$ is antisymmetric combination of excitation operators.

The MCSCF configuration space can be expressed as the unitary transformation between the reference state, $|0\rangle$, and the complementary space, $|k\rangle$, which spanned on $|0\rangle$ as

$$|k\rangle = \sum_{m}^{K} |m\rangle. \tag{2.23}$$

The unitary transformation is defined by projecting the reference state, $|0\rangle$, to the complementary space

$$\hat{S} = \sum_{K\neq 0} S_{K0}(|K\rangle\langle 0| - |0\rangle\langle K|) \tag{2.24}$$

where S_{K0} is the variational parameter and $\hat{S}^{\dagger} = -\hat{S}$. The unitary transformation of the reference state, $|0\rangle$, is obtained as

$$|0'\rangle = e^{\hat{S}}|0\rangle, \tag{2.25}$$

where the transformed function remains normalized. Thus, the overall transformation of the MCSCF wave function is

$$|0'\rangle = e^{\hat{T}}e^{\hat{S}}|0\rangle. \tag{2.26}$$

In equation (2.26), $\hat{T}$ and $\hat{S}$ do not commute. The energy of the system can be Taylor expanded over a stationary point p_i and for simplicity setting $p_0 = 0$ as

$$E(p) = E(0) + \sum_{i}\left(\frac{\partial E}{\partial p_i}\right)_0 p_i + \frac{1}{2}\sum_{i,j} p_i\left(\frac{\partial^2 E}{\partial p_i \partial p_j}\right)_0 p_j + \dots \tag{2.27}$$

or in vector notation

$$E(p) = E(0) + g^{\dagger}p + \frac{1}{2}p^{\dagger}Hp + \dots . \tag{2.28}$$

Here, g is the gradient vector and H is the Hessian matrix. The minimization of $E(p)$ is performed using the Newton-Raphson algorithm. Thus, the stationary point is obtained as the solutions to the equation; $\frac{\partial E}{\partial p_i} = 0$, which gives the set of linear equations

$$\begin{aligned} g + Hp &= 0 \\ p &= -H^{-1}g. \end{aligned} \tag{2.29}$$

These equations are solved iteratively until the convergence is reached. The energy expression for the wave function in (2.26) is given as

$$E(T,S) = \langle 0|e^{-\hat{S}}e^{-\hat{T}}\hat{H}e^{\hat{T}}e^{\hat{S}}|0\rangle. \tag{2.30}$$

By Taylor-expanding the equation (2.30) up to the second order terms of T and S, the energy formulation is expressed as

$$\begin{aligned} E(T,S) &= \langle 0|\hat{H} + [H,T] + [H,S] + \frac{1}{2}[[H,T],T] \\ &\quad + \frac{1}{2}[[H,S],S] + [[H,T],S] + \dots |0\rangle \\ &= E(0,0) + \sum_{i>j} T_{ij}\langle 0|[H,E_{ij}^{-}]|0\rangle + 2\sum_{K\neq 0} S_{K0}\langle 0|H|K\rangle \\ &\quad + \sum_{i>j} T_{ij}T_{kl}\big\{\langle 0|E_{ij}^{-}E_{kl}^{-}H|0\rangle + \langle 0|HE_{ij}^{-}E_{kl}^{-}|0\rangle \\ &\quad - 2\langle 0|E_{ij}^{-}HE_{kl}^{-}|0\rangle\big\} + 2\sum S_{K0}S_{L0}\big\{\langle K|H|L\rangle + \delta_{KL}\langle 0|H|0\rangle\big\} \\ &\quad + 2\sum S_{K0}T_{ij}\langle K|[H,E_{ij}^{-}]|0\rangle \\ &= E(0,0) + \sum T_{ij}g_{ij}^{(o)} + \sum S_{K0}g_{K}^{(c)} + \sum T_{ij}T_{kl}H_{ij,kl}^{oo} \\ &\quad + \sum S_{K0}S_{L0}H_{KL}^{cc} + \sum S_{K0}T_{ij}H_{K,ij}^{co}. \end{aligned} \tag{2.31}$$

The energy expansion in the equation (2.31) is equivalent to the equation (2.28). Similary, we obtained the set of the linear equations which is equivalent to the

equation (2.29) as

$$\begin{pmatrix} a & b \\ b^{\dagger} & c \end{pmatrix} \begin{pmatrix} S \\ T \end{pmatrix} = -\begin{pmatrix} v \\ w \end{pmatrix} \tag{2.32}$$

where the simplified notations are introduced as follows

$$a = \frac{1}{2}H^{cc}, b = \frac{1}{2}H^{co}, c = \frac{1}{2}H^{oo}, v = \frac{1}{2}g^{c}, w = \frac{1}{2}g^{o}.$$

The equation (2.32) is the MCSCF equation.

2.1.1 Complete Active Space SCF Method

Usually, the most difficult task in carrying out an MCSCF calculation is the selection of configuration space. For complicated molecules, the selection of a suitable configuration space can become very tedious.

There are several methods for selecting the MCSCF configurations. One of the successful approach is to partition the orbital space into three subspaces according to their occupation numbers (n_i) *i.e.* the *inactive* ($n_i = 2$), the *active* ($0 < n_i < 2$) and the *secondary* (*virtual*, $n_i = 0$) orbitals. This method is known as the *complete active space self-consistent field* (CASSCF). In this method, the MCSCF expansion is obtained by distributing the *active electrons* in all possible ways among the active orbitals. The active orbitals are normally orbitals which are involved in the bond-formation or the bond-dissociation of the molecule. The number of CAS configurations, N_{CAS}, can be calculated by the Weyl's formula:

$$N_{CAS} = \frac{2S+1}{n+1}\binom{n+1}{\frac{1}{2}N - S}\binom{n+1}{\frac{1}{2}N + S + 1} \tag{2.33}$$

where n is the number of molecular orbitals, N is the number of electrons ans S is the spin quantum number.

2.2 Configuration Interaction Theory

The typical applications of the CI method employ the Born-Oppenheimer approximation. Therefore, the electronic Schrödinger equation is solved at discrete sets of fixed nuclear positions

$$\begin{aligned}\hat{\mathrm{H}}_e\Psi_e(r;R) &= -\frac{1}{2}\sum_i \nabla_i^2 - \sum_{A,i}\frac{Z_A}{R_{Ai}} + \sum_{i>j}\frac{1}{r_{ij}}\Psi_e(r;R) \\ &= E_e(R)\Psi_e(r;R).\end{aligned} \tag{2.34}$$

It is important to remember that the electronic energy, E_e, is an artifact of the Born-Oppenheimer approximation and is not as physically meaningful as the total energy of the system. Within the Born-Oppenheimer approximation, we estimate the total energy by adding the nuclear-nuclear replusion energy to the total electronic energy, $U(R)$,

$$U(R) = E_e(R) + \sum_{A<B}\frac{Z_A Z_B}{R_{AB}}. \tag{2.35}$$

The configuration-interaction (CI) wave function consists of the linear combination of Slater determinants constituted the exact wave function

$$|\Phi_0\rangle = C_0|\Psi_0\rangle + \sum_{ar} C_a^r|\Psi_a^r\rangle + \sum_{a<b,r<s} C_{ab}^{rs}|\Psi_{ab}^{rs}\rangle + \ldots. \tag{2.36}$$

The CI method is the properly size-extensive, which will be discussed in more detailed in section 2.2.2. This method is flexible and highly accurate. However, it is applicable to small molecules only since the member of Slater determinants (configuration) to be included grows rapidly as the size of molecule increase and the calculation would become impossible to be carried out. Thus for large molecules, the CI expansion is normally truncated and the method is, therefore, susceptible to the size-extensive error or the lack thereof.

2.2.1 The CI model

In the CI method, the wave function is constructed as the linear combination of determinants or configuration state functions (CSFs)

$$|\mathbf{C}\rangle = \sum_i C_i |i\rangle \tag{2.37}$$

where the coefficient, C_i, is determined by variationally optimizing the expectation value of the electronic energy;

$$E_{CI} = \min_{\mathbf{C}} \frac{\langle \mathbf{C}|\hat{H}|\mathbf{C}\rangle}{\langle \mathbf{C}|\mathbf{C}\rangle}. \tag{2.38}$$

This condition is equivalent to a set of eigenvalue equations for the energy and the expansion coefficients

$$\mathbf{HC} = E_{CI}\mathbf{C} \tag{2.39}$$

where $\mathbf{H}$ is the Hamiltonian matrix with elements

$$H_{ij} = \langle i|\hat{H}|j\rangle \tag{2.40}$$

and $\mathbf{C}$ is the vector containing the expansion coefficient C_i. The equation (2.39) corresponds to a standard Hermitian eigenvalue problem of linear algebra.

In the CI expansion (2.37), the basis functions $|i\rangle$ are the Slater determinants. The wave function in the spin-symmetrized CSFs can be expanded more compact than Slater determinants. The linear transformation between CSFs asd Slater determinants of CI wave function can be carried out rather easily. The CSF expansions are adapted using the determinantal techniques by expanding the CSFs in determinants just before any calculation or manipulation is to be carried out on the CI wave function in transforming back again immediately afterwards. However, the high efficiency and generality, the simpler determinantal basis is more useful.

The CI method is completely general with respect to the choice of configuration. The *full CI (FCI) expansions* are the full set of determinants that generated by distributing all electrons among all orbitals.

For large system, the FCI wave function is very difficult to calculate. Thus, the truncation of FCI expansion is normally introduced. It is important to distinguish between static and dynamical correlation. The static correlation is treated by selecting the dominant configurations of the FCI expansion. These configurations are often referred to as the reference configurations of the CI wave function, and the spanning of these reference configurations is called the reference space. The dynamical correlation is treated by adding determinants constructed from excitations out of the reference space to the wave function. However, the number of configurations required in the CI expansion rise approximately as $(2K)^N$ so even a trivial FCI calculation is barely affordable. A more practical approach is to truncate the CI expansion and keep only terms up to the second summation (terms of double excitations) in (2.36). The calculation based on this approach is called *CI singles and doubles* (CISD)

2.2.2 Size-extensivity and the CI model

The simple model for the size-extensivity is the non-interacting of system, A and B. The FCI wave function for the system A can be written as

$$\begin{aligned} |\psi_A^{FCI}\rangle &= \hat{\psi}_A^{FCI}|vac\rangle \\ &= (\hat{\psi}_A^{HF} + \hat{\psi}_A^{corr})|vac\rangle \end{aligned} \tag{2.41}$$

where $\hat{\psi}_A^{HF}$ is the operator that generates the normalized Hartree-Fock reference state and $\hat{\psi}_A^{corr}$ is the operator that generates the correlation part of the wave

function. The FCI wave function satisfies the equation;

$$\hat{\mathbf{H}}_A|\psi_A^{FCI}\rangle = E_A^{FCI}|\psi_A^{FCI}\rangle \tag{2.42}$$

where $\hat{H}_A$ is the Hamiltonian of the system A. The FCI energy, E_A^{FCI}, can be seperated into the Hartree-Fock, E_A^{HF}, and the correlation energy, E_A^{corr},

$$E_A^{FCI} = E_A^{HF} + E_A^{corr} \tag{2.43}$$

$$E_A^{HF} = \langle\psi_A^{HF}|\hat{\mathbf{H}}_A|\psi_A^{HF}\rangle \tag{2.44}$$

$$E_A^{corr} = \frac{\langle\psi_A^{FCI}|\hat{\mathbf{H}}_A - E_A^{HF}|\psi_A^{FCI}\rangle}{\langle\psi_A^{FCI}|\psi_A^{FCI}\rangle}. \tag{2.45}$$

Similar equations hold for system B. The wave function of non-interaction system A and B is defined as

$$\begin{aligned}|\psi_{AB}^{FCI}\rangle &= \hat{\psi}_A^{FCI}\hat{\psi}_B^{FCI}|vac\rangle \\ &= (\hat{\psi}_A^{HF} + \hat{\psi}_A^{corr})(\hat{\psi}_B^{HF} + \hat{\psi}_B^{corr})|vac\rangle.\end{aligned} \tag{2.46}$$

The size-extensive solution for this system is represent as

$$(\hat{\mathbf{H}}_A + \hat{\mathbf{H}}_B)|\psi_{AB}^{FCI}\rangle = (E_A^{FCI} + E_B^{FCI})|\psi_{AB}^{FCI}\rangle \tag{2.47}$$

Because of the algebraic properties of the second-quantization the $\hat{\psi}_A^{FCI}$ and $\hat{\psi}_B^{FCI}$, the Pauli antisymmetry principle is satisfied for the product wave function $\hat{\psi}_A^{FCI}\hat{\psi}_B^{FCI}|vac\rangle$. The FCI wave function and energy of the compound system can now be expanded as

$$|\psi_{AB}^{FCI}\rangle = (\hat{\psi}_A^{HF}\hat{\psi}_B^{HF} + \hat{\psi}_A^{HF}\hat{\psi}_B^{corr} + \hat{\psi}_A^{corr}\hat{\psi}_B^{HF} + \hat{\psi}_A^{corr}\hat{\psi}_B^{corr})|vac\rangle \tag{2.48}$$

$$E_{AB}^{FCI} = E_A^{HF} + E_B^{HF} + E_A^{corr} + E_B^{corr}. \tag{2.49}$$

Since the Hartree-Fock energy $E_A^{HF} + E_B^{HF}$ is size-extensive, the FCI correlation energy $E_A^{corr} + E_B^{corr}$ must also be size-extensive. For the truncated CI wave function, the product $\hat{\psi}_A^{corr}\hat{\psi}_B^{corr}$ is not included. This exclusion of $\hat{\psi}_A^{corr}\hat{\psi}_B^{corr}$ leads to

the lack of size-extensivity in the truncated CI model. For examples, the truncated *CI-doubles* (CID) expansion, which contains the individual system $\hat{\psi}_A^{CID}$ and $\hat{\psi}_B^{CID}$ can be written in the form (2.41). Since the term $\hat{\psi}_A^{corr}\hat{\psi}_B^{corr}$, which contains quadruple excitations, is not included in the wave function for the non-interacting system. Thus, the truncated CID wave function for the system is written as

$$|\psi_{AB}^{CID}\rangle = (\hat{\psi}_A^{HF}\hat{\psi}_B^{HF} + \hat{\psi}_A^{HF}\hat{\psi}_B^{corr} + \hat{\psi}_A^{corr}\hat{\psi}_B^{HF})|vac\rangle \tag{2.50}$$

In this expression, $|\psi_{AB}^{CID}\rangle$ is constructed from the wave function of the subsystem A and B. Since the total energy can be written in terms of the size-extensive Hartree-Fock contribution

$$E_{AB}^{HF} = E_A^{HF} + E_B^{HF} \tag{2.51}$$

and the correlation contribution

$$E_{AB}^{corr} = \frac{\langle\psi_{AB}^{CID}|\hat{\mathbf{H}}_A + \hat{\mathbf{H}}_B - E_{AB}^{HF}|\psi_{AB}^{CID}\rangle}{\langle\psi_{AB}^{CID}|\psi_{AB}^{CID}\rangle}. \tag{2.52}$$

The expansion of the numerator in (2.52) for the correlation energy gives

$$\begin{aligned}\langle\psi_{AB}^{CID}|\hat{\mathbf{H}}_A + \hat{\mathbf{H}}_B - E_{AB}^{HF}|\psi_{AB}^{CID}\rangle &= \langle\psi_{AB}^{CID}|\hat{\mathbf{H}}_A - E_A^{HF}|\psi_{AB}^{CID}\rangle \\ &\quad + \langle\psi_{AB}^{CID}|\hat{\mathbf{H}}_B - E_B^{HF}|\psi_{AB}^{CID}\rangle\end{aligned} \tag{2.53}$$

Considering the first term in (2.53) and substituting the CID expression (2.50) then gives

$$
\begin{aligned}
\langle\psi_{AB}^{CID}|\hat{\mathbf{H}}_A - E_A^{HF}|\psi_{AB}^{CID}\rangle &= \langle vac|(\hat{\psi}_B^{HF\dagger}\hat{\psi}_A^{corr\dagger} + \hat{\psi}_B^{corr\dagger}\hat{\psi}_A^{HF\dagger} + \hat{\psi}_B^{HF\dagger}\hat{\psi}_A^{HF\dagger}) \\
&\quad (\hat{H}_A - E_A^{HF})(\hat{\psi}_A^{HF}\hat{\psi}_B^{HF} + \hat{\psi}_A^{HF}\hat{\psi}_B^{corr} \\
&\quad + \hat{\psi}_A^{corr}\hat{\psi}_B^{HF})|vac\rangle \\
&= \langle vac|\hat{\psi}_B^{HF\dagger}\hat{\psi}_A^{corr\dagger}(\hat{H}_A - E_A^{HF})\hat{\psi}_A^{HF}\hat{\psi}_B^{HF}|vac\rangle \\
&\quad + \langle vac|\hat{\psi}_B^{HF\dagger}\hat{\psi}_A^{corr\dagger}(\hat{H}_A - E_A^{HF})\hat{\psi}_A^{HF}\hat{\psi}_B^{corr}|vac\rangle \\
&\quad + \langle vac|\hat{\psi}_B^{HF\dagger}\hat{\psi}_A^{corr\dagger}(\hat{H}_A - E_A^{HF})\hat{\psi}_A^{corr}\hat{\psi}_B^{HF}|vac\rangle \\
&\quad + \langle vac|\hat{\psi}_B^{corr\dagger}\hat{\psi}_A^{HF\dagger}(\hat{H}_A - E_A^{HF})\hat{\psi}_A^{HF}\hat{\psi}_B^{HF}|vac\rangle \\
&\quad + \langle vac|\hat{\psi}_B^{corr\dagger}\hat{\psi}_A^{HF\dagger}(\hat{H}_A - E_A^{HF})\hat{\psi}_A^{HF}\hat{\psi}_B^{corr}|vac\rangle \\
&\quad + \langle vac|\hat{\psi}_B^{corr\dagger}\hat{\psi}_A^{HF\dagger}(\hat{H}_A - E_A^{HF})\hat{\psi}_A^{corr}\hat{\psi}_B^{HF}|vac\rangle \\
&\quad + \langle vac|\hat{\psi}_B^{HF\dagger}\hat{\psi}_A^{HF\dagger}(\hat{H}_A - E_A^{HF})\hat{\psi}_A^{HF}\hat{\psi}_B^{HF}|vac\rangle \\
&\quad + \langle vac|\hat{\psi}_B^{HF\dagger}\hat{\psi}_A^{HF\dagger}(\hat{H}_A - E_A^{HF})\hat{\psi}_A^{HF}\hat{\psi}_B^{corr}|vac\rangle \\
&\quad + \langle vac|\hat{\psi}_B^{HF\dagger}\hat{\psi}_A^{HF\dagger}(\hat{H}_A - E_A^{HF})\hat{\psi}_A^{corr}\hat{\psi}_B^{HF}|vac\rangle
\end{aligned}
\tag{2.54}
$$

Applying the orthogonal between $\hat{\psi}^{HF}$ and $\hat{\psi}^{corr}$ the expression (2.54) is reduced to

$$
\begin{aligned}
\langle\psi_{AB}^{CID}|\hat{\mathbf{H}}_A - E_A^{HF}|\psi_{AB}^{CID}\rangle &= \langle\psi_A^{corr}|\hat{H}_A - E_A^{HF}|\psi_A^{corr}\rangle + \langle\psi_A^{corr}|\hat{H}_A|\psi_A^{HF}\rangle \\
&\quad + \langle\psi_A^{HF}|\hat{H}_A|\psi_A^{corr}\rangle \\
&= \langle\psi_A^{CID}|\hat{H}_A - E_A^{HF}|\psi_A^{CID}\rangle
\end{aligned}
\tag{2.55}
$$

and similarly for the system B. Combining the formular such as (2.55) for the system A and B obtains

$$
\begin{aligned}
\langle\psi_{AB}^{CID}|\hat{\mathbf{H}}_A + \hat{\mathbf{H}}_B - E_{AB}^{HF}|\psi_{AB}^{CID}\rangle &= \langle\psi_A^{CID}|\hat{\mathbf{H}}_A - E_A^{HF}|\psi_A^{CID}\rangle \\
&\quad + \langle\psi_B^{CID}|\hat{\mathbf{H}}_B - E_B^{HF}|\psi_B^{CID}\rangle
\end{aligned}
\tag{2.56}
$$

The expansion of the denominator in (2.52) for the correlation energy yields

$$
\begin{aligned}
\langle\psi_{AB}^{CID}|\psi_{AB}^{CID}\rangle &= \langle vac|(\hat{\psi}_B^{HF\dagger}\hat{\psi}_A^{corr\dagger} + \hat{\psi}_B^{corr\dagger}\hat{\psi}_A^{HF\dagger} + \hat{\psi}_B^{HF\dagger}\hat{\psi}_A^{HF\dagger}) \\
&\quad (\hat{\psi}_A^{HF}\hat{\psi}_B^{HF} + \hat{\psi}_A^{HF}\hat{\psi}_B^{corr} + \hat{\psi}_A^{corr}\hat{\psi}_B^{HF})|vac\rangle \\
&= \langle vac|\hat{\psi}_B^{HF\dagger}\hat{\psi}_A^{corr\dagger}\hat{\psi}_A^{HF}\hat{\psi}_B^{HF}|vac\rangle \\
&\quad + \langle vac|\hat{\psi}_B^{HF\dagger}\hat{\psi}_A^{corr\dagger}\hat{\psi}_A^{HF}\hat{\psi}_B^{corr}|vac\rangle \\
&\quad + \langle vac|\hat{\psi}_B^{HF\dagger}\hat{\psi}_A^{corr\dagger}\hat{\psi}_A^{corr}\hat{\psi}_B^{HF}|vac\rangle \\
&\quad + \langle vac|\hat{\psi}_B^{corr\dagger}\hat{\psi}_A^{HF\dagger}\hat{\psi}_A^{HF}\hat{\psi}_B^{HF}|vac\rangle \\
&\quad + \langle vac|\hat{\psi}_B^{corr\dagger}\hat{\psi}_A^{HF\dagger}\hat{\psi}_A^{HF}\hat{\psi}_B^{corr}|vac\rangle \\
&\quad + \langle vac|\hat{\psi}_B^{corr\dagger}\hat{\psi}_A^{HF\dagger}\hat{\psi}_A^{corr}\hat{\psi}_B^{HF}|vac\rangle \\
&\quad + \langle vac|\hat{\psi}_B^{HF\dagger}\hat{\psi}_A^{HF\dagger}\hat{\psi}_A^{HF}\hat{\psi}_B^{HF}|vac\rangle \\
&\quad + \langle vac|\hat{\psi}_B^{HF\dagger}\hat{\psi}_A^{HF\dagger}\hat{\psi}_A^{HF}\hat{\psi}_B^{corr}|vac\rangle \\
&\quad + \langle vac|\hat{\psi}_B^{HF\dagger}\hat{\psi}_A^{HF\dagger}\hat{\psi}_A^{corr}\hat{\psi}_B^{HF}|vac\rangle \\
&= 1 + \langle\psi_A^{corr}|\psi_A^{corr}\rangle + \langle\psi_B^{corr}|\psi_B^{corr}\rangle \\
&= \langle\psi_A^{HF}|\psi_A^{HF}\rangle + \langle\psi_A^{corr}|\psi_A^{corr}\rangle + \langle\psi_B^{HF}|\psi_B^{HF}\rangle \\
&\quad + \langle\psi_B^{corr}|\psi_B^{corr}\rangle - 1 \\
&= \langle\psi_A^{CID}|\psi_A^{CID}\rangle + \langle\psi_B^{CID}|\psi_B^{CID}\rangle - 1.
\end{aligned}
\tag{2.57}
$$

Inserting the expanding of numerator (2.56) and denominator (2.57) in (2.52), we arrive at the following expression of the correlation energy of the truncated wave function:

$$
E_{AB}^{corr} = \frac{\langle\psi_{AB}^{CID}|\hat{\mathbf{H}}_A - E_A^{HF}|\psi_{AB}^{CID}\rangle + \langle\psi_{AB}^{CID}|\hat{\mathbf{H}}_B - E_B^{HF}|\psi_{AB}^{CID}\rangle}{\langle\psi_A^{CID}|\psi_A^{CID}\rangle + \langle\psi_B^{CID}|\psi_B^{CID}\rangle - 1}. \tag{2.58}
$$

The correlation energy of the truncated CID wave function (2.50) is not size-extensive. The expansion of the numerator and denominator in correlation energy (2.52) leads to a separation of the total energy as required by size-extensivity.

$$
E_{AB}^{corr^*} = \langle\psi_{AB}^{CID}|\hat{H}_A + \hat{H}_B - E_{AB}^{HF}|\psi_{AB}^{CID}\rangle \tag{2.59}
$$

For system A, consider the diference between the variational correlation energy (2.52) and the size-extensive correlation energy (2.59)

$$
E_A^{corr^*} - E_A^{corr} = \frac{\langle\psi_A^{CID}|\hat{H}_A - E_A^{HF}|\psi_A^{CID}\rangle}{1 + \langle\psi_A^{corr}|\psi_A^{corr}\rangle}\langle\psi_A^{corr}|\psi_A^{corr}\rangle \tag{2.60}
$$

The intermediately normalized CID wave function in (2.60) is proportional to the normalized state

$$|\psi_A^{CID}\rangle = C_0(|\psi_A^{HF}\rangle + |\psi_A^{corr}\rangle) \tag{2.61}$$

where

$$C_0 = \frac{1}{\sqrt{1 + \langle\psi_A^{corr}|\psi_A^{corr}\rangle}} \tag{2.62}$$

so the equation (2.60) express as

$$E_A^{corr^*} - E_A^{corr} = E_A^{corr}\frac{1 - C_0^2}{C_0^2}. \tag{2.63}$$

Since C_0^2 is assumed to be close to 1, then replace $\frac{1-C_0^2}{C_0^2}$ by $1 - C_0^2$ and (2.63) reduces to

$$E_A^Q = E_A^{corr}(1 - C_0^2). \tag{2.64}$$

This correction energy, E_A^Q, is the *Davidson correction.* However, the addition of the Davidson correction to the CI energy makes the energy only approximately size extensive. Because, the Davidson correction is determined from the cofficient of the calculation which is not size-extensive. Furthemore, this correction includes only contributions of quadruple excitations, while higher excitations are truncated.

2.2.3 CI Singles and Doubles method

The CISD method is based on the assumption that the wave function of the system can be well approximated by the Hartree-Fock determinant. For this assumption, the coefficient C_0 in (2.36) is much larger than other coefficients. The CI energy and also properties calculated are already near convergence by keeping only single and double excitations in the expansion (2.36). Since the CI equation

is a linear equation, it could be solved in a single step by diagonalizing the matrix H. However, the practical problem in calculation process is the number of operations and the storage of H. Therefore, the single step approach could put a severe limit on the CI energy calculation. The *direct CI* approach is introduced to solve the CI equation iteratively. In most cases, the CISD method is highly accurate for determination of energies and properties of molecules. The accuracy of this method depends on the satisfactory description of the Hartree-Fock wave function of the system, since the excitations include wave function out of Hartree-Fock space. Furthermore, the truncation of higher excitations in the CI expansion could cause the lack of *size-extensivity* (section 2.2.2). This error increases as the number of electrons in the system increases.

2.2.4 Multireference CI wave function

The multi-reference CI method (MRCI) would be an extension to MCSCF method. The wave function of MRCI is expressed by

$$|\Psi\rangle_{MRCI} = \sum_{\mu} \left[\mathrm{C}_{\mu}|\Psi_{\mu}\rangle + \sum_{ar} \mathrm{C}^{r}_{\mu a}|\Psi^{r}_{\mu a}\rangle + \sum_{a<b,r<s} \mathrm{C}^{rs}_{\mu ab}|\Psi^{rs}_{\mu ab}\rangle \right] \tag{2.65}$$

Similar to the CISD method, the CI expansion is truncated is keeping only single and double excitations. The first term of (2.65) is the MCSCF wave function. The single and double excitations is out of the MCSCF space. Similary to CISD, the direct CI approach also employed in the MRCI method to avoid the size problem and reduce the number of operations. One should also notice that the dimension of H (the member of CSFs) in the MRCI calculation is much larger than the CISD calculation.

The MRCI method is appropriate to treat the system with strong near-degeneracy

correlation, the configurations which is nearly degenerated to the Hartree-Fock state would also be important in the expansion. These configurations are not included in the CISD calculation. The error due to the size-extensivity of the MRCI calculation is smaller than that of the CISD calculation since large configurational space which contains higher excitations is included. This size-extensivity error can be further reduced by choosing larger reference spaces.

2.2.5 Direct CI methods

The crucial step in a CI calculation is the formation of the σ vector:

$$\sigma = HC \tag{2.66}$$

where C is a trial CI vector and H is the matrix Hamiltonain matrix:

$$\hat{H} = \sum_{p,q} h_{pq}\hat{E}_{pq} + \frac{1}{2}\sum_{p,q,r,s}(pq|rs)(\hat{E}_{pq}\hat{E}_{rs} - \delta\hat{E}_{ps}). \tag{2.67}$$

The σ vector is then:

$$\sigma_\mu = \sum_\nu \left[\sum_{p,q} h_{pq}A^{\mu\nu}_{pq} + \frac{1}{2}\sum_{p,q,r,s}(pq|rs)A^{\mu\nu}_{pqrs}\right]C_\nu \tag{2.68}$$

where $A^{\mu\nu}_{pq}$ and $A^{\mu\nu}_{pqrs}$ are the so-called direct CI coupling coefficients. Thus, instead of storing very large vectors such as $A^{\mu\nu}_{pq}$ and $A^{\mu\nu}_{pqrs}$ the problem is reduced to compute a much smaller vector σ_μ. This σ_μ could be computed as needed where no storage is required.

CHAPTER III

COMPUTATIONAL DETAILS

In this study, four systems which consisted of Fe_2, Fe_2^+, Fe_2^- and Fe_2^{++} were investigated. These are small systems, but have very complicated electronic structures with many low-lying states. Therefore, it would be most suitable to perform multi-reference CI (MRCI) calculations on these systems. Unfortunately, the success of the CI method depends on the starting orbitals since only CI coefficients are optimized. Usually, the starting orbitals of CI calculation is obtained from the optimized Hartree-Fock wave function. In normal CI calculations, the HF state is often chosen as the CI references state. In MRCI, the reference state must consist of multiple CSFs. Thus, it is natural to collect MCSCF's configurations as the reference state and its orbitals as the starting orbitals for MRCI calculations. The basis set employed in this study is *atomic natural orbital* (ANO) [$17s12p9d4f$] basis set of Pierloot et al. [14] For each system, the equilibrium nuclear (R_e) and zero-point frequency (ω_e) were determined. Furthermore, the first and the second ionization potential (IP) and the electron affinity of Fe_2 were computed from the energy difference between Fe_2 and its ionized states Fe_2^+, Fe_2^{++}, and Fe_2^-. All calculations were performed using the COLUMBUS [15, 16] program package.

3.1 COLUMBUS program package

The COLUMBUS package can perform serveral types of quantum chemical calculations. However, only procedures involving MCSCF and MRCI calculation were discussed.

3.1.1 MCSCF calculation

Firstly, input files for sucessive calculations must be created using *colinp* interface program. In colinp, informations such as geometry coordinates, molecular symmetry, number of electrons, spin multiplicity, basis functions etc. must be provided. Secondly, the *argos.x* program for evaluating one- and two-electron integrals over symmetry-adapted linear combinations of generally contracted gaussian atomic orbitals is launched. This program generates *argosls* as its list file and *aoints* and *aoints2* as integral files. Next, the *scfvie.x* which requires aoints and aoints2 to calculate restricted Hartree-Fock wave functions and energies may be executed. The scfvie.x yields *scfls* as printed output file and *mocoef* as molecular orbital coefficient file. This calculation is optional and it is useful for accelerating the convergence of the MCSCF calculation. The MCSCF requires guess molecular orbitals and formular to create CSFs. The former can be obtained from SCF calculation or previous run of MCSCF or core Hamiltonian while the latter is obtained by launching mcdrt.x and mcuft.x programs. The mcdrt.x could be run interactively or in the batch mode with *mcdrtin* as the input file. In this program, the molecular orbitals (MO) is catagorized to inactive, active and secondary orbitals (see section 2.1.1). This program constructs the distinct row table (DRT) which produces lists of CSFs while the mcuft.x generates the coupling coefficient over

active orbitals. The next step which is the final step is to carry out *mcscf.x* program. This program performs optimization of CFSs mixing coefficients and orbital expansion coefficients using the graphical unitary group approach and produces the MCSCF energy. The diagram describes the procedure concerning the MCSCF calculations depicted in Figure 1.

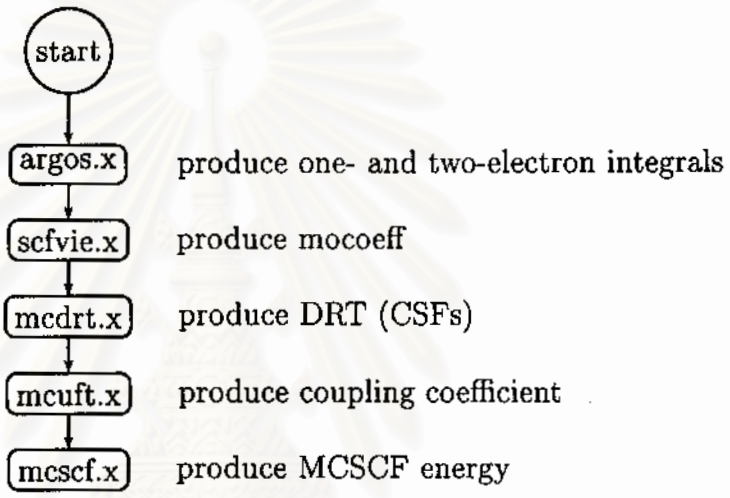

Figure 1: Schematic diagram of the MCSCF calculation

3.1.2 The CI calculation

To perform a CI calculation, the molecular orbital coefficient must be required. This could be done by taking mocoef obtained from scfvie.x or by transforming the restart file of mcscf.x to mocoef using *mofmt.x* program. As in the MCSCF calculation, the CI calculation required the DRT file which contains lists of CSFs. However, this DRT is different from that of mcscf since the input provides the definition of core, virtual, and internal orbitals as well as the reference state which is the list of selected CSFs. Normally, those given in the mcscf calculation will be chosen. This process performs using *cidrt.x* program. The efficiency of the wave

function optimization steps depends on the complexity of the DRT. In the case, where there are several ways of specifying a desired wave function, the best choice is the one that results in the smallest DRT and the shortest indexing vectors. Similar to mcscf, The *ciuft.x* program creates the diagonal formula file, *ciftdfl*, off-diagonal formula file, *ciftofl*, and information file, *ciftifl*. These files are needed in the next step. Afterwards, the one- and two-electron AO integrals must be transfromed to MO integrals using the *tran.x* program. For efficiency of the calculations, this transfromed MO integrals are sorted using *cisrt.x* program. After these preparation steps are completed, the *ciudg.x* program is launched and CI energy is obtained. Together with the CI energy, the Davidson corrections and simple wave function analysis are determined. The procedure for the CI calculation in diagram is given in Figure **2**.

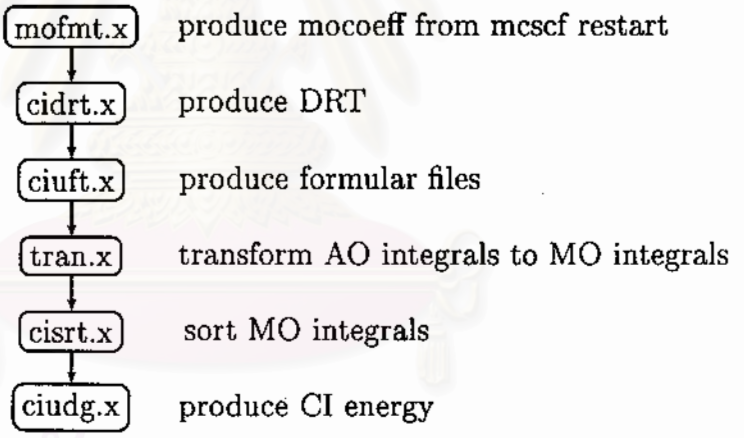

Figure **2**: Schematic diagram of the CI calculation

3.2 Basis set

Almlöf and Taylor [13] suggested the use of basis functions derived from the natural orbitals. The natural orbitals (NOs) are the one-electron representative of the many-electron wave function in which their corresponding eigenvalues, known as the occupation numbers, represent the contributions of different natural orbitals

to the many-electron density matrix. The NOs of the CISD wave function are truncated by occupation numbers to form a contracted set into desired size, and the expansion coefficients of the NOs in terms of the primitive basis functions then form the coefficient matrix for the general contraction. One advantage of this atomic NO approach is that a single uncontracted calculation provides the contraction information for any size of contracted set. The contracted sets are used in molecular calculation without further modification. This appoach is well defined and inexpensive, the natural orbital occupation numbers provide an excellent guide to the relative importance of each contracted function. Functions of higher angular quantum number than the highest occupied shell in the atom can be included in this approach without additional difficulty. In this study we employed the atomic natural orbitals (ANOs), which is the natural orbitals type basis set.

All calculations in this study were carried out using the modification of ANO Pierloot et al.'s [14] basis sets. The basis set used in these calculation consisted of $[17s12p9d]/(8s7p7d)$ denoted as 877 basis, $[17s12p9d4f]/(4s3p2d1f)$ basis denoted as 4321 basis, $[17s12p9d]/(5s4p3d)$ basis denoted as 543 basis, and $[17s12p9d4f]/(5s4p3d2f)$ basis denoted as 5432 basis.

3.3 The Fe_2 system

The molecular symmetry point group of Fe_2 molecule and Fe_2 molecule like ions are $D_{\infty h}$. Owing to the limitation of most electronic structure theoretical calculation programs, including the COLUMBUS program package, it is not pluasible to utilize molecular symmetry higher than the corresponding abelian group. Thus, the D_{2h} point group which is the sub group of the $D_{\infty h}$ symmetry is imposed. The term symbols of molecular states of Fe_2 in the $D_{\infty h}$ symmetry which adapted to the

D_{2h} symmetry were given in Table **2**. The electonic ground state of Fe_2 molecule is experimentally determined to be the $^7\Delta_u$ state. [5, 7, 8] For performing the MCSCF calculations, molecular orbitals of the Fe_2 must be divided into inactive (with occupations $n_i = 2$), active (with $0 < n_i < 2$), and unoccupied (with $n_i = 0$) orbitals. Thus, 18 orbitals ($1s\sigma_g$ to $3p\pi_g$) obtained from the linear combinations of $1s$ to $3p$ orbitals of 2 Fe atoms were selected as the inactive orbitals. For the active space, 12 orbitals from the linear combinations of $3d$ and $4s$ orbitals of 2 Fe atoms were chosen. The rest are unoccupied orbitals. The sketch of the active space which consisted of 16 electrons in 12 orbitals were shown in Figure **3**. Since the molecular state for investigation is $^7\Delta_u$ state, the B_{1u} molecular symmetry (a D_{2h} representative of Δ_u symmetry) was chosen. Using the active space in Figure **3** and restricting to B_{1u} symmetry, 1,150 CSFs of MCSCF were generated. For CI calculations, MCSCF's CSFs with CI coefficient > 0.05 and its MO were selected as the CI reference and starting vectors respectively.

Table 2: The irreducible representation of D_{2h} symmetry of MO of Fe_2 like structure.

AO interaction	MO type	Irrep. of D_{2h}
$1s - 1s$	$1\sigma_g$, $1\sigma_u$	a_g, b_{1u}[a]
$2s - 2s$	$2\sigma_g$, $2\sigma_u$	a_g, b_{1u}
$2p_z - 2p_z$	$3\sigma_g$, $3\sigma_u$	a_g, b_{1u}
$2p_x - 2p_x$, $2p_y - 2p_y$	$1\pi_u$, $1\pi_g$	$(b_{3u}, b_{2g}), (b_{2u}, b_{3g})$
$3s - 3s$	$4\sigma_g$, $4\sigma_u$	a_g, b_{1u}
$3p_z - 3p_z$	$5\sigma_g$, $5\sigma_u$	a_g, b_{1u}
$3p_x - 3p_x$, $3p_y - 3p_y$	$2\pi_u$, $2\pi_g$	$(b_{3u}, b_{2g}), (b_{2u}, b_{3g})$
$3d_{z^2} - 3d_{z^2}$	$6\sigma_g$, $6\sigma_u$	a_g, b_{1u}
$3d_{xz} - 3d_{xz}$, $3d_{yz} - 3d_{yz}$	$3\pi_u$, $3\pi_g$	$(b_{3u}, b_{2g}), (b_{2u}, b_{3g})$
$3d_{xy} - 3d_{xy}$, $3d_{x^2-y^2} - 3d_{x^2-y^2}$	$1\delta_g$, $1\delta_u$	$(b_{1g}, a_u), (a_g, b_{1u})$
$4s - 4s$	$4s\sigma_g$, $4s\sigma_u$	a_g, b_{1u}

[a]bonding, anti-bonding

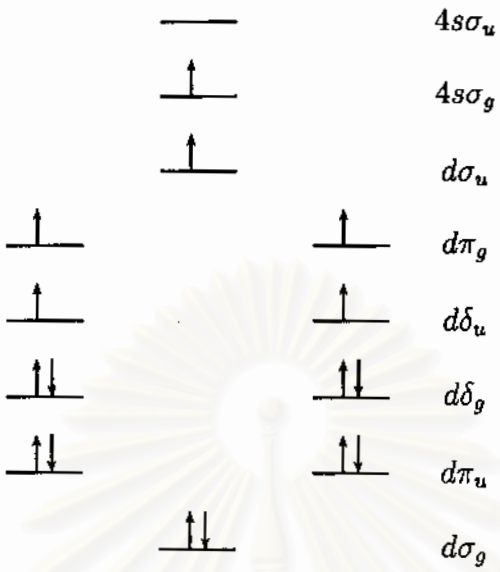

Figure 3: Possible electron configuration of Fe_2 molecule and rough sketch of its active space.

3.4 The Fe_2^+ system

Since Fe_2^+ is very similar to Fe_2 except there is one electron less, the same inactive, active and unoccupied spaces were imposed. The corresponding representatives in D_{2h} of Δ_u are A_u and B_{1u} symmetries. However, A_u is also representative for Σ_u. Thus B_{1u} is chosen. The $^8\Delta_u$ state was suggested as the electronic ground state of Fe_2^+ by Tatewaki et al. [18] The possible electron configuration and sketch of the active space which consisted of 15 electrons in 12 active orbitals were given in Figure 4. A similar procedure to that of Fe_2 for selecting CI reference and starting vectors is performed for Fe_2^+.

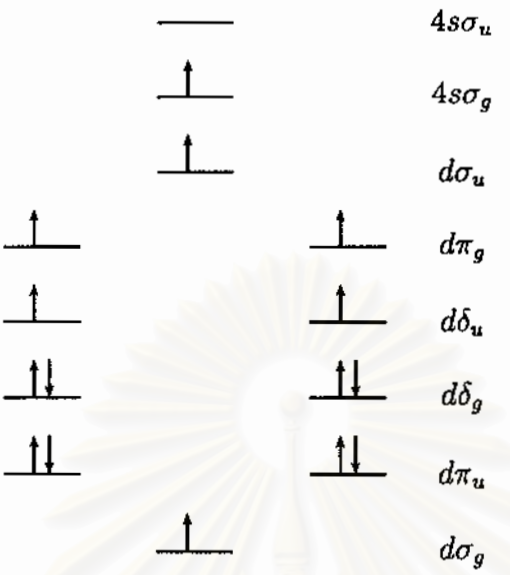

Figure 4: Possible electron configuration of Fe_2^+ molecule and rough sketch of its active space.

3.5 The Fe_2^- system

The corresponding D_{2h} representatives for the Δ_g state are B_{1g} and A_g. By similar argument to Fe_2^+ system, the B_{1g} is chosen. The spaces as in the cases of Fe_2 and Fe_2^+ were imposed. From previous studies, $^8\Delta_g$ state was suggested as the electronic ground state of Fe_2^-. [4, 8] The possible electron configuration and the sketch of the active space which consisted of 17 electrons in 12 active orbitals were demonstrated in Figure 5.

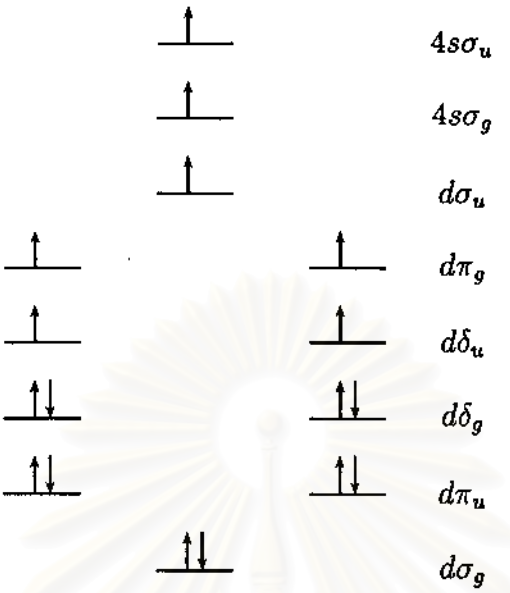

Figure 5: Possible electron configuration of Fe_2^- molecule and rough sketch of its active space.

3.6 The Fe_2^{++} system

Experimental and theoretical suggestions on the electronic structure of Fe_2^{++} are still lacked. Hence, there is no prior knowledge on the ground state of Fe_2^{++}, calculations on several possible states were performed and their corresponding energies were compared. Then, the ground state can be suggested. However, there are too many possible states to be considered. Using the knowledge from the ground electronic structure of Fe_2^+, 4 possible states were selected for Fe_2^{++}. The Fe_2^+ has the $(3d\sigma_g)^1(3d\pi_u)^4(3d\delta_g)^2(3d\delta_u)^2(3d\pi_g)^2(3d\sigma_u)^1(4s\sigma_g)^1$ configuration for the valence electrons and $4s$ electrons have lower energy that $3d$ electrons. Therefore, only the states which resulted from the detachment of $3d$ electrons were considered. For the linear molecule, $3d$ orbitals can combine to form molecular orbitals which can be classified as sigma type ($3d\sigma$), pi type ($3d\pi$), and delta

type ($3d\delta$). (In each orbital types, there exists a bonding and an anti-bonding orbital denoted by the subscript g and u.) Among the d orbital types, the $3d\sigma$ has the lowest energy. Thus, only states derived from the detachment of an electron in $3d\pi$ and $3d\delta$ are investigated. Taken a β-electron from $3d\delta_g$, the $^9\Delta_u$ state is formed. This state corresponds to ^9A_u and $^9B_{1u}$ states in D_{2h}. By similar argument to the previous sections, the $^9B_{1u}$ state was studied. Taken a β-electron from $3d\pi_u$, the $^9\Pi_g$ state is formed. In D_{2h}, this state is split to $^9B_{2g}$ and $^9B_{3g}$ states and we selected $^9B_{3g}$ to study. By detaching one electron from $3d\delta_u$, the $^7\Delta_g$ which is represented by ^7A_g and $^7B_{1g}$ in D_{2h} symmetry is obtained. The $^7B_{1g}$ was chosen for the calculations. Finally $^7\Pi_u$ state is resulted when ionizing one electron from $3d\pi_u$ orbital. This state is decomposed to $^7B_{2u}$ and $^7B_{3u}$ state in D_{2h} and only $^7B_{3u}$ was considered. The MCSCF and MRCI calculations on the 4 states *i.e.* $^9\Delta_u$ ($^9B_{1u}$), $^9\Pi_g$ ($^9B_{3g}$), $^7\Delta_g$ ($^7B_{1g}$), and $^7\Pi_u$ ($^7B_{3u}$) were carried out. The active space similar to other Fe_2 systems which contains 14 electrons in 12 active orbitals was imposed. The MCSCF orbitals and CSFs with coefficient larger than 0.05 were used as starting vectors and CI reference in the MRCI calculations. The equilibrium distance (R_e), the harmonic frequency (ω_e) of these 4 state were determined and their energies were then compared.

CHAPTER IV

RESULTS AND DISCUSSION

4.1 Fe_2

Experimentally, the R_e obtained in inert gas matrix [2, 3] and ω_e obtained from the resonance Raman spectrum [19, 20] of Fe_2 molecule are 3.54-3.82 Bohr and 299.6 cm^{-1} respectively. In this study, the electronic and molecular structure of Fe_2 molecule in the $^7\Delta_u$ state (the ground electronic state) were investigated using 4 basis sets i.e. 877, 4321, 543 and 5432 (see section 3.2).

4.1.1 Electronic structure

As mentioned in section 1.1, there were several theoretical studies on the electronic and molecular structure of Fe_2 and the most accepted work is that of Tomonari and Tatewaki. In this study (see Table 3), we obtained the CSF#2 as the main configuration with contribution to the total wave function is only 53.9%. Thus, it would not be reasonable to use the CSF#2 as a sole representative for the electronic structure of Fe_2 due to the multi-determinantal nature of the wave function. In this case, the natural occupations which is the average occupations of all CSFs would be used as the better representative and the electronic structure of Fe_2 obtained from the natural occupations is $(3d\sigma_g)^{1.7}$ $(3d\sigma_u)^{1.2}$ $(3d\pi_u)^{3.5}$ $(3d\pi_g)^{2.4}$ $(3d\delta_g)^{3.7}$ $(3d\delta_u)^{2.3}$ $(4s\sigma_g)^{1.0}$ $(4s\sigma_u)^{0.0}$.

Table 3: Electronic configurations with coefficients of the main configurations obtained from calculation carried out with 5432 basis of Fe_2 molecule.

CSF	coefficient	$d\sigma_g$	$d\sigma_u$	$d\pi_g$	$d\pi'_g$	$d\pi_u$	$d\pi'_u$	$d\delta_g$	$d\delta'_g$	$d\delta_u$	$d\delta'_u$	$4s\sigma_g$	$4s\sigma_u$
1	0.115591	2	2	1	1	1	1	2	2	1	2	1	0
2	-0.734011	2	1	1	1	2	2	2	2	1	1	1	0
3	-0.215473	2	1	2	1	2	1	2	1	1	2	1	0
4	0.112913	2	1	2	1	1	2	2	1	2	1	1	0
5	0.215472	2	1	1	2	1	2	2	1	1	2	1	0
6	-0.112913	2	1	1	2	2	1	2	1	2	1	1	0
7	0.138580	1	1	2	1	1	2	2	2	1	2	1	0
8	-0.182056	1	1	2	1	2	1	2	2	2	1	1	0
9	-0.062391	1	2	2	1	2	1	2	2	1	1	1	0
10	-0.138580	1	1	1	2	2	1	2	2	1	2	1	0
11	0.182056	1	1	1	2	1	2	2	2	2	1	1	0
12	0.263202	1	1	2	2	1	1	2	1	2	2	1	0

From this electronic structure, the bond order was calculated and the value of 2.00 was resulted. The natural occupations obtained from this calculations together with those from other calculations were listed in Table 4.

Table 4: The natural occupations of CI calculation of Fe_2 with 5432 basis.

									bond order		
	$d\sigma_g$	$d\sigma_u$	$d\pi_u$	$d\pi_g$	$d\delta_g$	$d\delta_u$	$4s\sigma_g$	$4s\sigma_u$	$3d$	$4s$	total
5432	1.7	1.2	3.5	2.4	3.7	2.3	1.0	0.0	1.50	0.50	2.00
Shim et al.	1.6	2.5	3.1	2.9	2.5	2.5	2.0	0.0	-0.35	1.00	0.65
Harris et al.	2.0	1.0	4.0	2.0	3.0	2.0	2.0	0.0	2.00	1.00	3.00
Tomonari at al.	1.9	1.1	3.7	2.3	2.8	2.2	2.0	0.0	1.40	1.00	2.40

By decomposing the bond order into the contribution of $3d$ and $4s$ orbitals, it appears that the $3d$ contribute to 76% of the bond, while it is only 24% for the $4s$. When categorizing by bond characters, the Fe-Fe bond comprises of 44% σ, 27% π, and 29% δ, while the σ character is almost 50% $3d$ and 50% $4s$. The main electron configuration of Fe_2 from Tomonari and Tatewaki's were shown in Table 5. In their calculations, they chose $3d\sigma^3 3d\pi^6 3d\delta^5 4s\sigma^2$ as the reference state

for CI calculations and kept $4s\sigma$ as the core orbital (always doubly occupied). This reference state, however, contributes to 64% of the total wave function. From the natural occupations (Table 4), the configuration for Fe_2 is $(3d\sigma_g)^{1.9}$ $(3d\sigma_u)^{1.1}$ $(3d\pi_u)^{3.7}$ $(3d\pi_g)^{2.3}$ $(3d\delta_g)^{2.8}$ $(3d\delta_u)^{2.2}$ $(4s\sigma_g)^{2.0}$ $(4s\sigma_u)^{0.0}$.

Table 5: RCSFs of the valence CI for Fe_2 of Tomonari.

CSF	$d\sigma_g$	$d\sigma_u$	$d\pi_g$	$d\pi'_g$	$d\pi_u$	$d\pi'_u$	$d\delta_g$	$d\delta'_g$	$d\delta_u$	$d\delta'_u$	$4s\sigma_g$	$4s\sigma_u$
RCSF 1	2	1	2	1	1	2	1	1	2	1	2	0
RCSF 2	2	1	1	2	2	1	1	1	2	1	2	0
RCSF 3	2	1	1	2	1	2	1	1	1	2	2	0
RCSF 4	2	1	2	1	2	1	1	1	1	2	2	0
RCSF 5	1	2	2	1	1	2	2	1	1	1	2	0
RCSF 6	1	2	1	2	2	1	2	1	1	1	2	0
RCSF 7	1	2	1	2	1	2	1	2	1	1	2	0
RCSF 8	1	2	2	1	2	1	1	2	1	1	2	0
RCSF 9	2	1	2	2	1	1	1	2	1	1	2	0
RCSF 10	2	1	1	1	2	2	1	2	1	1	2	0
RCSF 11	1	2	2	2	1	1	1	1	1	2	2	0
RCSF 12	1	2	1	1	2	2	1	1	1	2	2	0
RCSF 13	1	1	2	2	2	2	1	1	1	1	2	0

Interestingly, both the main configuration and natural occupations from Tomonari and Tatewaki's and ours are quite different. From analysis of the natural occupations, it was found that the Fe-Fe has the total bond order of 2.40, which is slightly stronger than that in our suggestions. This Fe-Fe bond has 58% contribution from $3d$ and 42% from $4s$. Analysis by bond types, it is 58% σ, 29% π and 12.5% δ. Therefore, Tomonari's Fe-Fe bond has less $3d$ contribution and is more σ characteristic which comes mainly from $4s$. Again, one could see right away that the Fe-Fe bond as suggested by Tomonari and Tatewaki and us are markedly different. This difference is possibly caused by the discrepancy of the electronic structure obtained from the calculations.

Considering the work of Shim and Gingerich and Harris and Jones, their nat-

ural occupations appear to be different from ours and Tomonari and Tatewaki's. Harris and Jones predicted too strong Fe-Fe bond (bond order of 3.00). This is probably due to the nature of DFT calculation which uses single-determinantal wave function. Shim and Gingerich, however, suggested too weak bond with antibonding $3d$, although they employed the SCF-CI scheme similar to ours and Tomonari and Tatewaki's. It seems that the choice of CI reference state and guess vectors does has an effect on the CI results.

4.1.2 Molecular structure

Using 877, 4321, 543, and 5432 basis, the MRCI energies at nuclear distances from 3.80-4.40 Bohr with the interval of 0.1 Bohr were given in Table **6**. The potential plot of the energy relative to the minimum of the result in Table **6** were shown in Figure **6**. From the plot, then the harmonic model was applied and the equilibrium nuclear distance (R_e), the energies at minimum (TE), and the zero-point frequencies (ω_e) at different level of basis set were yielded and listed in Table **7**. From Table **6**, the 543 basis gave the result with the highest total energy. By saturating s, p, and d functions of 543 basis (877 basis), the energies is improved by 22 mHartree (energies being compared at R = 2.40 Bohr). Interestingly, by including two f function to the 543 basis (5432 basis), its energy decreases by 143 mHartree (a 6.5 fold compared to when s, p, d were saturated). This implies that the inclusion of functions with higher angular momentum (such as f, g, h functions) is necessary. Thus, the 5432 basis seems to be sufficiently large for the Fe_2 molecule and further investigations based on this basis set are warranted. Comparing R_e and ω_e obtained at various basis sets, the 877 gave the shortest R_e of 4.14 Bohr but also the lowest ω_e of 309.7 cm^{-1}. The 5432 basis gave comparable

R_e (4.15 Bohr) to that of 877 and a reasonably ω_e of 215.0 cm^{-1}.

Table 6: The calculation energy results of CI and CI energy (Hartree) with correction calculated of the Fe_2 molecule. [a]

877 basis					
Distance	ECI	ECI+Q	ECI+Q2	ECI+Q3	ECI+pople
3.80	-0.04295	-0.09204	-0.10010	-0.11132	-0.09976
3.90	-0.04587	-0.09453	-0.10256	-0.11377	-0.10227
4.00	-0.04689	-0.09375	-0.10130	-0.11175	-0.10085
4.10	-0.04786	-0.09311	-0.10024	-0.11003	-0.09965
4.20	-0.04781	-0.09150	-0.09823	-0.10740	-0.09752
4321 basis					
Distance	ECI	ECI+Q	ECI+Q2	ECI+Q3	ECI+pople
3.80	-0.08681	-0.13452	-0.14111	-0.14982	-0.13968
3.90	-0.08988	-0.13723	-0.14380	-0.15249	-0.14240
4.00	-0.09106	-0.13698	-0.14323	-0.15146	-0.14178
4.10	-0.09169	-0.13612	-0.14204	-0.14979	-0.14053
4.20	-0.09193	-0.13497	-0.14059	-0.14789	-0.13902
4.30	-0.09183	-0.13360	-0.13894	-0.14585	-0.13733
4.40	-0.09143	-0.13206	-0.13716	-0.14372	-0.13551
4.50	-0.09077	-0.13039	-0.13528	-0.14154	-0.13360
543 basis					
Distance	ECI	ECI+Q	ECI+Q2	ECI+Q3	ECI+pople
3.90	-0.02262	-0.06986	-0.07790	-0.08925	-0.07785
4.00	-0.02442	-0.07004	-0.07764	-0.08827	-0.07742
4.10	-0.02543	-0.06939	-0.07653	-0.08645	-0.07616
4.20	-0.02589	-0.06829	-0.07502	-0.08429	-0.07451
4.30	-0.02591	-0.06683	-0.07317	-0.08184	-0.07255
4.40	-0.02554	-0.06509	-0.07108	-0.07920	-0.07035
5432 basis					
Distance	ECI	ECI+Q	ECI+Q2	ECI+Q3	ECI+pople
3.80	-0.16431	-0.22304	-0.23150	-0.24280	-0.23003
3.90	-0.16765	-0.22664	-0.23527	-0.24684	-0.23390
4.00	-0.16859	-0.22615	-0.23444	-0.24552	-0.23300
4.10	-0.16906	-0.22503	-0.23294	-0.24345	-0.23141
4.20	-0.16904	-0.22348	-0.23103	-0.24100	-0.22941

[a] -2524.0 Hartree is added to the total energy.

Compared to experimental results of 3.54-3.82 Bohr for R_e and 299.6 cm^{-1}

for ω_e, it appears that the 877 basis generally yielded a better result. The better agreement might cause by the cancellation of error and the values from 5432 basis should then be accepted. It is well known that the CI result could be seriously affected by the size-extensive error or the lack thereof. One attempt to correct the size-extensive error is the Davidson's correction (Q) as discussed in section 2.2.2. Table 7 shows the R_e and ω_e obtained without and with consideration of size-extensive correction to CI. Also, in the Table, listed R_e and ω_e reported by previous studies and experiments. By inclusion of size-extensive correction, the R_e is shorten and the value closer to the experiment was obtained.

Table 7: The MRCI results of Fe_2 calculate with 877, 4321, 543, and 5432 basis set.

	R_e (Bohr)	TE (Hartree)	ω_e (cm^{-1})
877 basis			
CI	4.14	-2525.04786	309.7
CI+Q	3.99	-2525.09534	406.6
4321 basis			
CI	4.27	-2525.09202	212.0
CI+Q	4.01	-2525.13826	404.3
543 basis			
CI	4.26	-2525.02588	202.2
CI+Q	3.97	-2525.07007	279.9
5432 basis			
CI	4.15	-2525.16911	215.0
CI+Q	3.96	-2525.22708	453.6
Expt.	3.82 or 3.53	-	299.6
Tominari	3.82	-	448.5
Shim	4.54	-	204.0

However, the ω_e of CI+Q methods are much too high when compared to the experiment. This means that the CI+Q gave too deep potential which results in a shorter bond lenght and stronger Fe-Fe bond. This, however, is possibly the artifact of the size-extensive correction methods. Although, our calculations gave longer R_e to that of Tomonari and Tatewaki, the calculated ω_e is closer

to the experiment (215.0 cm^{-1} compared with 448.5 cm^{-1} from Tomonari and Tatewaki [8]). Whereas, the R_e reported by Shim and Gingerich [7] is too large when compared to the experiment. Interestingly, the calculated R_e from the three calculations, Tomonari and Tatewaki, ours, and Shim and Gingerich depend on the bond order (Fe-Fe longer as the bond order becomes smaller). Thus, the electronic structure dictates the molecular structure of Fe_2. To assess the quality of the calculation, one could not rely on the agreement with R_e alone. The agreement with ω_e should also be considered, since the more accurate method should also produce the correct curvature (ω_e) of the potential plot. Using this argument, we are quite confident in our results and the correct description of the Fe-Fe bond should be as we have suggested.

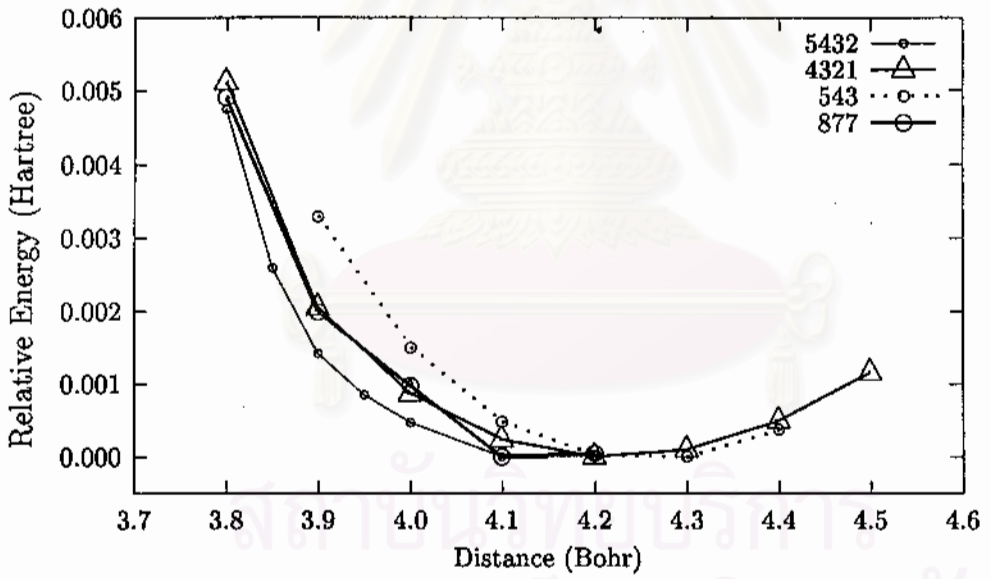

Figure 6: The represent data of Fe_2 molecule calculated based on 5432 basis

4.2 Fe_2^+

The electronic ground state for Fe_2^+ as suggested by Tatewaki et al. [18] is $^8\Delta_u$ and the R_e of 4.91 Bohr (2.60 Å) was reported.

4.2.1 Electronic structure

In this study (see Table 8), the CSF#3 is the main configuration with the contribution to the total wave function of 62,2%. The natural occupations assessment produces the $(3d\sigma_g)^{1.0}$ $(3d\sigma_u)^{1.0}$ $(3d\pi_u)^{3.5}$ $(3d\pi_g)^{2.4}$ $(3d\delta_g)^{3.6}$ $(3d\delta_u)^{2.3}$ $(4s\sigma_g)^{1.0}$ $(4s\sigma_u)^{0.1}$ configuration for the $^8\Delta_u$ state of Fe_2^+. Compared to the $^7\Delta_u$ state of Fe_2, this state is the result of the deletion of one electron from the bonding $3d\sigma_g$. Thus, the weakening of Fe-Fe bond is expected. This reflects by the reduced total bond order of 1.65 as compared to 2.00 in Fe_2.

Table 8: Electronic configurations with coefficients of the main configurations obtained from calculation carried out with 5432 basis of Fe_2^+ molecule.

CSF	coefficient	$d\sigma_g$	$d\sigma_u$	$d\pi_g$	$d\pi'_g$	$d\pi_u$	$d\pi'_u$	$d\delta_g$	$d\delta'_g$	$d\delta_u$	$d\delta'_u$	$4s\sigma_g$	$4s\sigma_u$
1	0.110441	1	1	2	2	1	1	2	2	1	1	1	0
2	0.121219	1	1	1	1	1	1	2	2	2	2	1	0
3	0.788809	1	1	1	1	2	2	2	2	1	1	1	0
4	0.285720	1	1	2	1	2	1	2	1	1	2	1	0
5	-0.285719	1	1	1	2	1	2	2	1	1	2	1	0
6	-0.138855	1	1	2	2	1	1	1	1	1	2	1	$\bar{1}^a$

[a] $\bar{1} \equiv \beta$ spin

Table 9: The natural occupations of CI calculation of Fe_2^+ with 5432 basis.

									bond order		
	$d\sigma_g$	$d\sigma_u$	$d\pi_u$	$d\pi_g$	$d\delta_g$	$d\delta_u$	$4s\sigma_g$	$4s\sigma_u$	$3d$	$4s$	total
5432	1.0	1.0	3.5	2.4	3.6	2.3	1.0	0.1	1.20	0.45	1.65

The 1.65 bond order compries of 27% σ, 33% π, and 40% δ. The σ bond comes from $4s$ orbital completely. From the bond order, the lenghtening of the bond is evident due to the high percentage of the weaker δ bond.

4.2.2 Molecular structure

The MRCI energies at nuclear distance between 4.00-5.00 Bohr with the interval of 0.10 Bohr obtained using 4321 and 5432 basis were given in Table **10**.

Table **10**: The MRCI and CI+Q energies computed at various nuclear distances using 4321 and 5432 basis of the $^8\Delta_u$ state Fe_2^+. [a]

4321 basis					
Distance	ECI	ECI+Q	ECI+Q2	ECI+Q3	ECI+pople
4.20	-0.88355	-0.92799	-0.93450	-0.94325	-0.93287
4.30	-0.88583	-0.93004	-0.93651	-0.94519	-0.93488
4.40	-0.88726	-0.93130	-0.93774	-0.94639	-0.93611
4.50	-0.88798	-0.93192	-0.93835	-0.94699	-0.93674
4.60	-0.88813	-0.93204	-0.93848	-0.94714	-0.93688
4.70	-0.88784	-0.93177	-0.93824	-0.94695	-0.93666
5432 basis					
Distance	ECI	ECI+Q	ECI+Q2	ECI+Q3	ECI+pople
4.40	-0.98621	-1.03984	-1.04779	-1.05852	-1.04590
4.50	-0.98637	-1.03996	-1.04796	-1.05876	-1.04611
4.60	-0.98602	-1.03981	-1.04789	-1.05883	-1.04608

[a] -2524.0 Hartree is added to the total energy.

The R_e, TE and ω_e computed at 4321 and 5432 basis and the R_e obtained from Tatewaki et.al. were listed in Table **11**. The results of CI+Q were also included in Table **11**. The R_e from both 4321 and 5432 basis and CI+Q calculations are all agreed to the value around 4.50 Bohr. However, their corresponding ω_e's are varied. The ω_e from 4321 basis is too large compared to when using 5432 basis. The much longer R_e (4.50 Bohr) of Fe_2^+ compared to that of Fe_2 (4.15 Bohr) suggests a weaker Fe-Fe bond in this case. Thus, the smaller ω_e than 250 cm^{-1} should be expected. The ω_e between 159-219 cm^{-1} as obtained from CI and CI+Q methods with 5432 basis seems to fit into this estimation.

Table 11: The MRCI results of Fe_2^+ calculate with the 4321 and the 5432 basis set.

	R_e (Bohr)	TE (Hartree)	ω_e (cm^{-1})
4321 basis			
CI	4.49	-2524.88798	406.4
CI+Q	4.50	-2524.93192	328.0
5432 basis			
CI	4.48	-2524.98638	219.4
CI+Q	4.49	-2525.03996	159.6
Tatewaki	4.91	-	-

Unfortunately, there is no experimental R_e and ω_e for Fe_2^+ to compare with our calculations. The only experimental evidence that exists is the first ionization potential (IP_1) in which the comparison to our calculations is shown in Table **12**. Thus, our calculations is in good agreement with the experiment IP and the size-extensive correction scheme improved the calculated IP by 0.13 eV.

Table 12: The first ionization potential of 4321 and 5432 with any corelation.

	IP_1 (eV)
4321	4.35
5432 (CI)	4.97
5432 (CI+Q)	5.09
5432 (CI+Q2)	5.11
5432 (CI+Pople)	5.12
Tomonari et al.	4.79
Experimental	6.30±0.01

The 4321 basis yields too weak ionization, which probaply due to the underestimated of Fe_2 energy. The agreement with experimented IP increases the confidence in the calculated R_e and ω_e obtained from our calculations, therefore, it is reasonable too say that the R_e of 4.90 Bohr as reported by Tatewaki might be too long

and for Fe_2^+ the R_e should be around 4.5 Bohr with ω_e between 150.0-219.0 cm^{-1}.

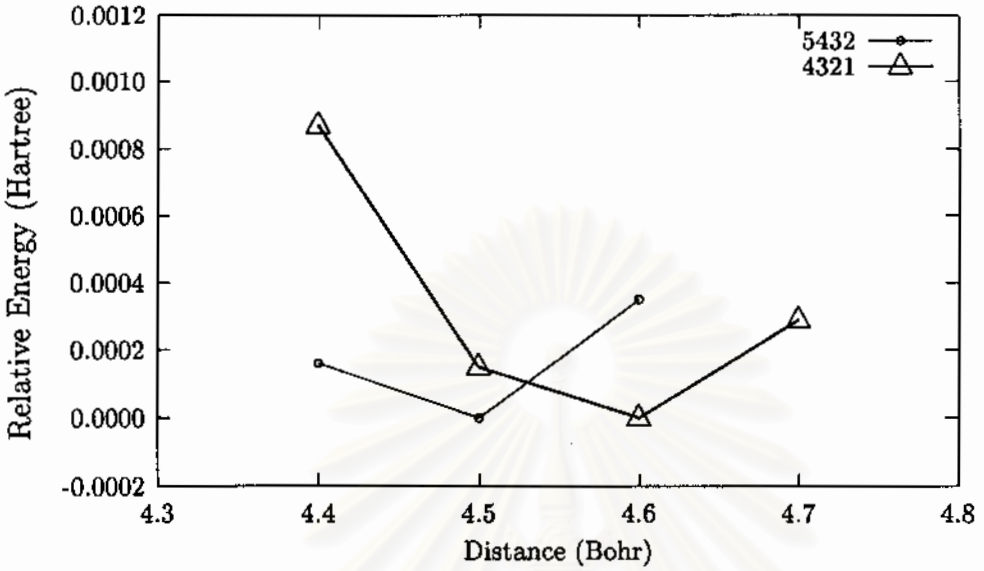

Figure 7: The represent data of Fe_2^+ molecule calculated based on 5432 basis

4.3 Fe_2^-

For Fe_2^-, the experimental data reported by Leopold and Lineberger [4] gave the R_e and the ω_e of 3.89-4.04 Bohr and 250 ± 20 cm^{-1}, respectively. The electronic ground state that is suggested by Tatewaki et al. [18] is $^8\Delta_g$. They also reported the R_e and the ω_e for Fe_2^- of 3.88 Bohr (2.05 Å) and 370 cm^{-1}, respectively. Their calculated R_e is in the range of the experiments. However, their calculated ω_e is overestimated. Here, MRCI calculations using 4321 and 5432 basis were carried out for Fe_2^-.

4.3.1 Electronic structure

Tomonari and Tatewaki suggested electron configurations of Fe_2^- similar to those of $^7\Delta_u$ state of Fe_2 (see Table 5), except that the $4s\sigma_g^2$ occupation was re-

placed by $4s\sigma_g^2 4s\sigma_u^1$. In our calculations, the electron configurations were chosen according to Leopold and Lineberger's result [4] which suggested an extra electron in $4s\sigma_u$. The obtained electron configurations, which displayed in Table **13**, especially the main configuration is the same as those of $^7\Delta_u$ state Fe_2 (see Table **3**), except there is an extra electron in $4s\sigma_u$.

Table **13**: Electronic configurations with coefficients of the main configurations obtained from calculation carried out with 5432 basis of Fe_2^- molecule.

CSF	coefficient	$d\sigma_g$	$d\sigma_u$	$d\pi_g$	$d\pi'_g$	$d\pi_u$	$d\pi'_u$	$d\delta_g$	$d\delta'_g$	$d\delta_u$	$d\delta'_u$	$4s\sigma_g$	$4s\sigma_u$
1	0.145727	2	2	1	1	1	1	2	2	1	2	1	1
2	0.681582	2	1	1	1	2	2	2	2	1	1	1	1
3	0.226666	2	1	2	1	2	1	2	1	1	2	1	1
4	0.124189	2	1	2	1	1	2	2	1	2	1	1	1
5	-0.226668	2	1	1	2	1	2	2	1	1	2	1	1
6	-0.124189	2	1	1	2	2	1	2	1	2	1	1	1
7	0.108205	1	1	1	1	1	1	2	2	2	2	2	1
8	-0.171764	1	1	2	1	1	2	2	2	1	2	1	1
9	-0.193580	1	1	2	1	2	1	2	2	2	1	1	1
10	0.171764	1	1	1	2	2	1	2	2	1	2	1	1
11	0.193579	1	1	1	2	1	2	2	2	2	1	1	1
12	0.300181	1	1	2	2	1	1	2	1	2	2	1	1

Obviously, as in the case of $^7\Delta_u$ state of Fe_2, these configurations differ from those reported by Tomonari and Tatewaki's. Again, the leading configuration contributes only 46% of the total wave function. Thus, the wave function is heavily multi-configurational. Its electronic structure should then be represented by the natural occupations and the $(3d\sigma_g)^{1.7}$ $(3d\sigma_u)^{1.2}$ $(3d\pi_u)^{3.3}$ $(3d\pi_g)^{2.5}$ $(3d\delta_g)^{3.7}$ $(3d\delta_u)^{2.4}$ $(4s\sigma_g)^{1.0}$ $(4s\sigma_u)^{1.0}$ configuration was obtained. This configuration is very similar to those of $^7\Delta_u$ state Fe_2 except the additional occupation of 1.0 at $4s\sigma_u$. This configuration results in the total bond order of 1.30, a much smaller value as compared to the Fe-Fe bond in Fe_2. Similar trend is also observed by Tomonari and Tatewaki. The weakening of the Fe-Fe bond is caused by the occupation of the additional electron to the antibonding $4s\sigma_u$ orbital. However, our calculations

suggested that bonding of Fe-Fe contributes totally by $3d$. From our result, the contributions by σ, π, and δ are almost equal.

Table **14**: The natural occupations of CI calculation of Fe_2^- with 5432 basis.

									bond order		
	$d\sigma_g$	$d\sigma_u$	$d\pi_u$	$d\pi_g$	$d\delta_g$	$d\delta_u$	$4s\sigma_g$	$4s\sigma_u$	$3d$	$4s$	total
5432	1.7	1.2	3.3	2.5	3.7	2.4	1.0	1.0	1.30	0.00	1.30

4.3.2 Molecular structure

Table **15** shows MRCI energies using 4321 and 5432 basis at the nuclear distances from 3.80 to 4.50 Bohr with the interval of 0.1 Bohr. The potential plot of energies according to 4321 and 5432 basis were displayed in Figure **8**. The values in Table **15** were used to calculated R_e, TE, and ω_e using the harmonic model. The results were given in Table **16**. In addition, the R_e, the TE, and the ω_e calculated using the size-extensive correction scheme (CI+Q) were also included. For the CI+Q at 5432 basis, the R_e of 4.03 Bohr and ω_e of 278.2 cm^{-1} were resulted. For 5432 basis (without correction), a longer R_e of 4.37 Bohr and a smaller ω_e of 140.8 cm^{-1} were yielded. The size-extensive correction seems to deepen the potential curve which causes a shorter bond and larger ω_e. The 4321's R_e of 4.03 agrees with the CI+Q but its ω_e is too large. Besides there is an irregularity in the potential curve of this basis (Figure **8**). Therefore, the 4321 result should be disregarded.

Table 15: The calculation energy results of CI and CI energy (Hartree) with correction calculated of the Fe_2^- molecule. [a]

4321 basis					
Distance	ECI	ECI+Q	ECI+Q2	ECI+Q3	ECI+pople
3.80	-0.06360	-0.11764	-0.12582	-0.13692	-0.12550
3.90	-0.06568	-0.11847	-0.12636	-0.13701	-0.12595
4.00	-0.07008	-0.12125	-0.12873	-0.13878	-0.12818
4.10	-0.06892	-0.11973	-0.12717	-0.13716	-0.12663
4.20	-0.06970	-0.11915	-0.12626	-0.13576	-0.12562
4.30	-0.06955	-0.11709	-0.12373	-0.13252	-0.12294
5432 basis					
Distance	ECI	ECI+Q	ECI+Q2	ECI+Q3	ECI+pople
3.90	-0.17511	-0.23799	-0.24767	-0.26086	-0.24744
4.00	-0.17721	-0.23865	-0.24797	-0.26062	-0.24762
4.10	-0.17853	-0.23849	-0.24744	-0.25952	-0.24696
4.20	-0.17897	-0.23819	-0.24696	-0.25876	-0.24642
4.30	-0.17963	-0.23669	-0.24492	-0.25592	-0.24420
4.40	-0.17967	-0.23540	-0.24330	-0.25382	-0.24248
4.50	-0.17950	-0.23399	-0.24160	-0.25168	-0.24069

[a] -2524.0 Hartree is added to the total energy.

Table 16: The MRCI results of Fe_2^- calculate with the 4321 and the 5432 basis set.

	R_e (Bohr)	TE (Hartree)	ω_e (cm^{-1})
4321 basis			
CI	4.03	-2525.07032	724.4
CI+Q	4.01	-2525.12130	637.1
5432 basis			
CI	4.37	-2525.17968	140.8
CI+Q	4.03	-2525.23869	278.2
Tomonari et al.	3.88		370.0
Expt.	3.89 - 4.04		250±20

The R_e and ω_e of CI+Q methods are within the experimental error which reflects the quality of our calculations. However, when considered the experimen-

tal electron affinities (EA), see Table **17**, our best estimation is underestimated by 0.529 eV, the value which is unsatisfactory though Tomonari and Tatewaki's estimation does not fair much better (EA = 0.450 eV).

Table **17**: Electron affinity of result of Fe_2 by MRCI.

	EA (eV)
4321	-0.590
5432 (CI)	0.288
5432 (CI+Q)	0.316
5432 (CI+Q2)	0.337
5432 (CI+Pople)	0.365
Tomonari et al.	0.450
Experimental	0.902±0.008

Interestingly, the negative EA were obtained when using 4321 basis this implies the lower energy of Fe_2 as compared to Fe_2^- which is very unlikely for most cases since the electronic energy varies with numbers of electrons. Thus, the result reflects the dificiency of 4321 basis on the calculations of Fe_2^-. This deficiency is probably caused by the extra electron in Fe_2^-. This suggested that the 5432 basis might still be insufficient for the calculation of Fe_2^-. The energy could be lowered by inclusion of additional *s, p, d, f* functions or by adding functions with higher angular momentum. Thus, the computed EA could be improved by using larger basis sets while the R_e and the ω_e would not very much affected. Comparing the slightly lenghtening of the bond (for 3.86 in Fe_2 to 4.04 in Fe_2^-) with the reduced bond order to that of Fe_2^+, the mismatch should be noticed. Probably, the elongation of Fe-Fe bond in Fe_2^+ is caused by the repulsion of extra charges on Fe atom and the discrepancy of the bond order between Fe_2^+ and Fe_2^- is explained.

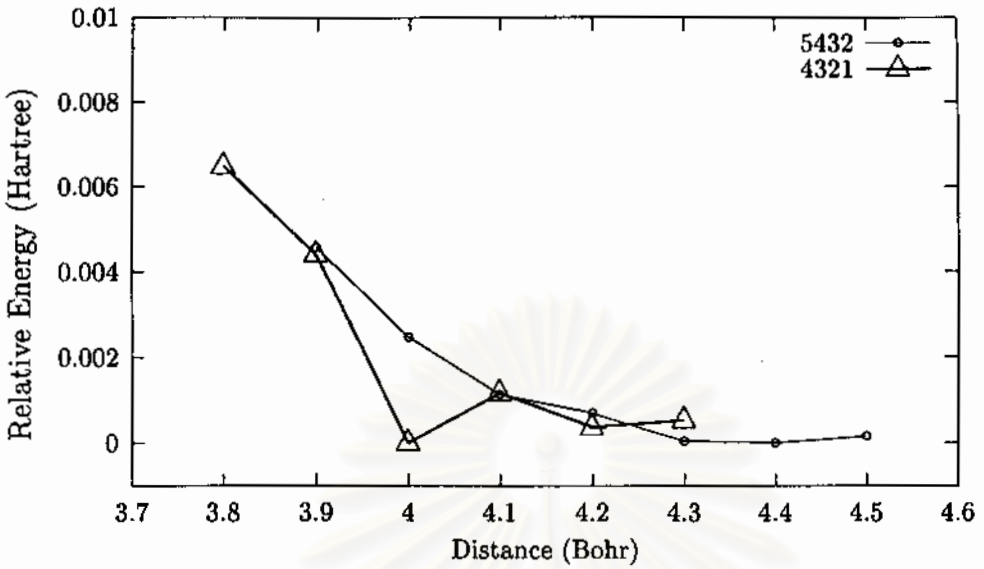

Figure 8: The represent data of Fe_2^- molecule calculated based on 5432 basis

4.4 Fe_2^{++}

As discussed in section 3.6, only 4 state *i.e.* $^9\Delta_u$, $^9\Pi_g$, $^7\Delta_g$, and $^7\Pi_u$ state were considered. Unlike the previous systems, their is no information experimentally and theoretically regarding the electronic and molecular structures for the Fe_2^{++}. Since the the ionization of Fe_2 molecule both 1st and 2nd order are of interest, one aim of this work is, therefore, to find out the second ionization potential (IP_2). This would require the knownledge of the electronic and molecular structure of Fe_2^{++}. Hence, the electronic ground state of Fe_2^{++} were sought. MRCI calculations for various state of Fe_2^{++} were carried out using 5432 basis. Their minimum energies were searched to elucidate the ground state of Fe_2^{++}.

4.4.1 The $^9\Delta_u$ state

The MRCI configurations with coefficients larger than 0.1 of $^9\Delta_u$ state Fe_2^{++} were listed in Table **18**. The leading configuration has 52% weight of the wave function. The configurations in Table **18** is very similar to that of Fe_2^+ (see Table **8**) except one electron less. Furthermore, the CSF#2 has the same configuration as the leading configuration of the Fe_2^+ substracting one electron from $3d\sigma_g$ orbital. The natural occupations for the $^9\Delta_u$ state, is $(3d\sigma_g)^{1.0}$ $(3d\sigma_u)^{1.1}$ $(3d\pi_u)^{3.4}$ $(3d\pi_g)^{2.4}$ $(3d\delta_g)^{2.7}$ $(3d\delta_u)^{2.3}$ $(4s\sigma_g)^{1.0}$ $(4s\sigma_u)^{0.0}$. The MRCI energies and their corresponding CI+Q at nuclear distances from 5.60 to 6.10 Bohr with the interval of 0.1 Bohr were given in Table **19**.

Table **18**: Electronic configurations with coefficients of the main configurations obtained from calculation carried out with 5432 basis of Fe_2^{++} molecule, $^9\Delta_u$.

CSF	coefficient	$d\sigma_g$	$d\sigma_u$	$d\pi_g$	$d\pi'_g$	$d\pi_u$	$d\pi'_u$	$d\delta_g$	$d\delta'_g$	$d\delta_u$	$d\delta'_u$	$4s\sigma_g$	$4s\sigma_u$
1	0.235499	1	1	1	1	1	1	1	2	2	2	1	0
2	0.722320	1	1	1	1	2	2	1	2	1	1	1	0
3	0.318165	1	1	2	1	2	1	1	1	1	2	1	0
4	-0.121231	1	2	2	1	1	2	1	1	1	1	1	0
5	-0.316519	1	1	1	2	1	2	1	1	1	2	1	0
6	0.120804	1	2	1	2	2	1	1	1	1	1	1	0

Table **19**: The CI energies (-2524.0 + x Hartree) at various nuclear distances calculated with 5432 basis.

Distance	ECI	ECI+Q	ECI+Q2	ECI+Q3	ECI+pople
5.60	-0.38172	-0.44996	-0.46399	-0.48530	-0.46380
5.70	-0.38174	-0.45032	-0.46452	-0.48611	-0.46440
5.80	-0.38167	-0.45065	-0.46502	-0.48694	-0.46499
5.90	-0.38154	-0.45095	-0.46551	-0.48780	-0.46558
6.00	-0.38139	-0.45127	-0.46605	-0.48875	-0.46623
6.10	-0.37311	-0.43349	-0.44510	-0.46223	-0.44420

From Table **19**, R_e, TE, and ω_e were then computed and given in table **26**. A

very long R_e of 5.67 (CI) and 5.95 (CI+Q) Bohr with corresponding ω_e of 92.2 and 1307.0 cm^{-1} were reported. The very dubious value of 1307.0 cm^{-1} for ω_e reflectd the irregularity of the CI+Q method.

4.4.2 The $^9\Pi_g$ state

The MRCI configurations of $^9\Pi_g$ state Fe_2^{++} were listed in Table 20. Since this is quite different state from $^9\Delta_u$ state, the electron configuration in Table 20 is markedly different from those in Table 18. They are two leading configurations with the weight of 44 and 37%. Thus, both contribute to 81% of total wave function. From the natural occupations analysis, the electronic structure of $^9\Pi_g$ state is given as $(3d\sigma_g)^{1.0}$ $(3d\sigma_u)^{1.0}$ $(3d\pi_u)^{2.5}$ $(3d\pi_g)^{2.4}$ $(3d\delta_g)^{3.5}$ $(3d\delta_u)^{2.4}$ $(4s\sigma_g)^{1.0}$ $(4s\sigma_u)^{0.0}$. This configuration is similar to that of $^7\Delta_u$ state of Fe_2 by deleting one electron from $3d\pi_u$ and one from $3d\delta_u$.

Table 20: Electronic configurations with coefficients of the main configurations obtained from calculation carried out with 5432 basis of Fe_2^{++} molecule, $^9\Pi_g$.

CSF	coefficient	$d\sigma_g$	$d\sigma_u$	$d\pi_g$	$d\pi'_g$	$d\pi_u$	$d\pi'_u$	$d\delta_g$	$d\delta'_g$	$d\delta_u$	$d\delta'_u$	$4s\sigma_g$	$4s\sigma_u$
20	0.666136	1	1	1	1	1	2	2	2	1	1	1	0
26	-0.609248	1	1	2	1	1	1	2	1	1	2	1	0
128	0.220363	1	1	1	1	1	2	1	2	1	1	2	0
134	-0.160122	1	1	2	1	1	1	1	1	1	2	2	0

Table **21**: The CI energies (-2524.0 + x Hartree) at various nuclear distances calculated with 5432 basis.

Distance	ECI	ECI+Q	ECI+Q2	ECI+Q3	ECI+pople
4.00	-0.38236	-0.41510	-0.41899	-0.42393	-0.41660
4.50	-0.41521	-0.44476	-0.44818	-0.45250	-0.44596
5.00	-0.42989	-0.45452	-0.45709	-0.46026	-0.45504
5.10	-0.43092	-0.45496	-0.45743	-0.46047	-0.45541
5.20	-0.43146	-0.45501	-0.45741	-0.46035	-0.45541
5.30	-0.43159	-0.45473	-0.45707	-0.45993	-0.45509
5.40	-0.43136	-0.45417	-0.45646	-0.45925	-0.45450
5.50	-0.43081	-0.45336	-0.45561	-0.45836	-0.45367
6.00	-0.42868	-0.44848	-0.45030	-0.45249	-0.44849

MRCI and CI+Qs energies at nuclear distances from 4.00 to 6.00 Bohr with the interval of 0.1 Bohr were shown in Table **21**. Their corresponding R_e and ω_e were summarized in Table **26** and the values of 5.29 (CI) and 5.16 (CI+Q) for R_e were reported as well as ω_e of 140.3 (CI) and 116.4 (CI+Q) cm^{-1}.

4.4.3 The $^7\Delta_g$ state

The MRCI configurations of $^7\Delta_g$ state displayed in Table **22**. There are only two configurations with CI coefficient larger than 0.1. These configurations contribute to only 41% of the total wave function. This implies that the wave function is highly multi-configurational. The electron configuration for the $^7\Delta_g$ state derived from the natural occpations is $(3d\sigma_g)^{1.0}$ $(3d\sigma_u)^{1.0}$ $(3d\pi_u)^{3.1}$ $(3d\pi_g)^{2.9}$ $(3d\delta_g)^{3.2}$ $(3d\delta_u)^{1.8}$ $(4s\sigma_g)^{1.0}$ $(4s\sigma_u)^{0.0}$. Comparing with the ground state of Fe_2, this state is obtained by detaching one electron from $3d\delta_g$ and one from $3d\delta_u$.

Table **22**: Electronic configurations with coefficients of the main configurations obtained from calculation carried out with 5432 basis of Fe_2^{++} molecule, $^7\Delta_g$.

CSF	coefficient	$d\sigma_g$	$d\sigma_u$	$d\pi_g$	$d\pi'_g$	$d\pi_u$	$d\pi'_u$	$d\delta_g$	$d\delta'_g$	$d\delta_u$	$d\delta'_u$	$4s\sigma_g$	$4s\sigma_u$
145	0.427881	1	1	2	2	1	1	2	2	1	0	1	0
198	0.480304	1	1	1	1	2	2	2	2	1	0	1	0

Table **23**: The CI energies (-2524.0 + x Hartree) at various nuclear distances calculated with 5432 basis.

Distance	ECI	ECI+Q	ECI+Q2	ECI+Q3	ECI+pople
3.90	-0.15610	-0.34778	-0.43456	-0.66491	-0.49138
4.00	-0.17309	-0.36311	-0.45166	-0.69475	-0.51184
4.10	-0.18614	-0.37867	-0.47305	-0.74887	-0.54132
4.50	-0.25995	-0.53309	-0.81434	-0.25995	+1.72154
5.00	-0.27490	-0.57044	-0.93472	-0.27490	+1.73958
5.20	-0.27697	-0.57861	-0.96662	-0.27697	+1.74081
5.30	-0.27736	-0.58169	-0.98020	-0.27736	+1.74061
5.40	-0.27739	-0.58422	-0.99247	-0.27739	+1.73995
5.50	-0.27709	-0.58624	-1.00355	-0.27709	+1.73891
5.60	-0.27650	-0.58782	-1.01358	-0.27650	+1.73754
6.00	-0.27194	-0.59063	-1.04479	-0.27194	+1.72962

Table **23** shows MRCI and CI+Qs energies at the distance from 3.90 to 6.00 Bohr with the interval of 0.1 Bohr of the $^7\Delta_u$ state. The R_e and the ω_e obtained from these values were given in Table **26** in which R_e of 5.36 Bohr and ω_e of 176.5 cm^{-1} were listed. Interestingly for those CI+Qs no minimum could be located within the range of nuclear distances studied. Thus, the CI+Qs results are not reliable for this system.

4.4.4 The $^7\Pi_u$ state

The MRCI configurations of the $^7\Pi_u$ state are given in Table **24**. This configurations contribute to 82.4% of the total wave function while the leading term is

42.9%. Thus, this state is not as highly multi-configurational as the $^7\Delta_g$ state. From the natural occupations, this state has the configuration of $(3d\sigma_g)^{2.0}$ $(3d\sigma_u)^{2.0}$ $(3d\pi_u)^{2.9}$ $(3d\pi_g)^{2.0}$ $(3d\delta_g)^{2.0}$ $(3d\delta_u)^{2.0}$ $(4s\sigma_g)^{1.0}$ $(4s\sigma_u)^{0.0}$. The formation of this state is quite complicated. Compared to the $^7\Delta_u$ of Fe_2, 2 electrons is removed from the $3\delta_u/3\delta_g$ orbitals while there is a promotion of one electron from the $3d\pi_u/3d\pi_g$ orbitals to $3d\sigma_u$ or vice versa.

Table **24**: Electronic configurations with coefficients of the main configurations obtained from calculation carried out with 5432 basis of Fe_2^{++} molecule, $^7\Pi_u$.

CSF	coefficient	$d\sigma_g$	$d\sigma_u$	$d\pi_g$	$d\pi'_g$	$d\pi_u$	$d\pi'_u$	$d\delta_g$	$d\delta'_g$	$d\delta_u$	$d\delta'_u$	$4s\sigma_g$	$4s\sigma_u$
382	0.655460	2	1	0	2	2	1	1	1	2	1	1	0
386	0.384375	2	2	0	2	2	1	1	1	1	1	1	0
666	0.432282	1	1	0	2	2	1	1	1	2	1	2	0
670	0.248059	1	2	0	2	2	1	1	1	1	1	2	0

Table **25**: The CI energies (-2524.0 + x Hartree) at various nuclear distances calculated with 5432 basis.

Distance	ECI	ECI+Q	ECI+Q2	ECI+Q3	ECI+pople
4.00	-0.14813	-0.35492	-0.44499	-0.67408	-0.50100
4.50	-0.25711	-0.51869	-0.77692	-40.99595	-1.10901
5.00	-0.27110	-0.56366	-0.91685	-0.27110	+1.73619
5.30	-0.27357	-0.57498	-0.96177	-0.27357	+1.73730
5.40	-0.27361	-0.57752	-0.97388	-0.27361	+1.73666
5.50	-0.27332	-0.57956	-0.98482	-0.27332	+1.73565
6.00	-0.26825	-0.58398	-1.02515	-0.26825	+1.72658

The Table **25** displays the MRCI and CI+Qs energies of the $^7\Pi_u$ state at the nuclear distances from 4.00 to 6.00 Bohr with the interval of 0.1 Bohr.The R_e of 5.36 Bohr and ω_e of 176.5 cm^{-1} deduced from the information in Table **25** were given in Table **26**. Again, no minimum could be observed within this range of nuclear distances for CI+Qs methods. Thus, these methods do not provide reliable results.

4.4.5 The ground state of Fe_2^{++}

The comparison of R_e, ω_e, and energy difference (ΔE) of four states of Fe_2^{++} calculated using MRCI methods and 5432 basis were given in Table **26**.

Table **26**: R_e, ω_e, TE, and ΔE of different states of Fe_2^{++} computed at MRCI level and 5432 basis.

	R_e (Bohr)	TE (Hartree)	ω_e (cm^{-1})	ΔE (kcal/mol)
$^9\Delta_u$ state				
CI	5.67	-2524.38174	92.2	31.28
CI+Q	5.95	-2524.45338	1307.0	
$^9\Pi_g$ state				
CI	5.29	-2524.43159	184.3	0.00
CI+Q	5.16	-2525.45503	176.4	
$^7\Delta_g$ state				
CI	5.36	-2524.27742	176.5	96.74
CI+Q	-	-	-	
$^7\Pi_u$ state				
CI	5.36	-2524.27363	176.5	99.12
CI+Q	-	-	-	

Among the four states, the $^9\Pi_g$ has the lowest energy following by the $^9\Delta_u$, $^7\Delta_g$, and $^7\Pi_u$ state which are 31.28, 96.74, and 99.12 kcal/mol higher in energy, respectively. The $^9\Pi_g$ state is, therefore, the ground state of Fe_2^{++}. The potential plot of the 4 states were given in Figure 9. The ground state of Fe_2^{++} has the R_e of 5.29 Bohr and ω_e of 176.5 cm^{-1}. The Fe-Fe bond in Fe_2^{++} has the total bond order of 1.10, where the main contribution comes from σ and π bond. Thus, Fe_2^{++} has the weakest bond among all Fe_2 systems. However, the Fe-Fe bond seems to be too long as compared to its bond order. This is probably due to the repulsion of charges that bear on each Fe atom. From the CI and CI+Q minimum energies, the second ionization potential could be calculated and the value of 15.1 (CI) and 15.9 (CI+Q) eV were obtained. This suggests the much stronger binding of electron to

Fe_2^+ as compared to the Fe_2 (~6.3 eV) Therefore, it would be very unlikely for Fe_2 to form the bi-cationic state.

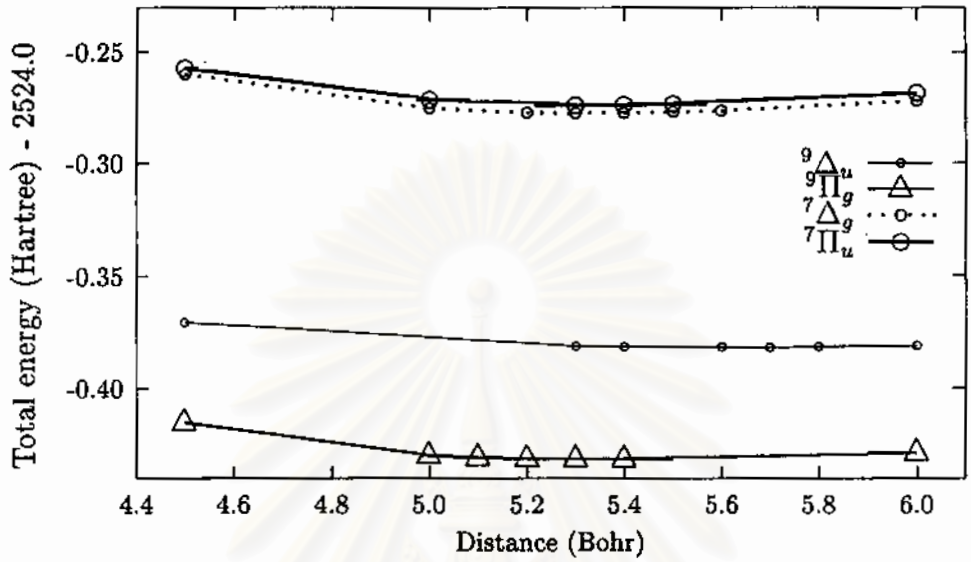

Figure 9: The represent data of Fe_2^{++} molecule calculated based on 5432 basis.

CHAPTER V

CONCLUSION

This thesis investigated the electronic and molecular structure of the ground states of Fe_2, Fe_2^+, Fe_2^- and Fe_2^{++} with MCSCF-MRCI calculation. Our best approximation predicted the equlibrium nuclear distance (R_e) and the zero-point frequency (ω_e) for Fe_2 of 3.96 Bohr and 453.6 cm^{-1} respectively. This compares well with the experimental R_e and the ω_e of 3.54-3.82 Bohr [2, 3] and 299.6 cm^{-1}, respectively and also in good agreement with the prediction of Tomonari et al. However, there is markedly difference between the electron configuration of our calculations and that of Tomonari et al. Our calculations yield the electron configuration of $((3d\sigma_g)^{1.7}\ (3d\sigma_u)^{1.2}\ (3d\pi_u)^{3.5}\ (3d\pi_g)^{2.4}\ (3d\delta_g)^{3.7}\ (3d\delta_u)^{2.3}\ (4s\sigma_g)^{1.0}\ (4s\sigma_u)^{0.0})$ with the bond order of 2.00 and the Fe-Fe bond comprises with 37.5% σ, 27.5% π, and 35.0% δ bonds, while the Fe-Fe bond predicted by Tomonari et al. has the bond order of 2.40 which comprises of 58.3% σ, 29.2% π, and 12.5% δ. Indeed, our Fe-Fe bond and that of Tomonari and Tatewaki are quite different. For the Fe_2^+ molecule, the electronic ground state is $^8\Delta_u$ state. The R_e and the ω_e obtained using the 5432 basis are 4.49 Bohr and 159.6 cm^{-1}, compared to Tatewaki et al. [18] whose R_e is 4.91 Bohr. For the $^8\Delta_u$ state of Fe_2^+, the occupation numbers of the natural orbitals revealed the electronic configuration of $((3d\sigma_g)^{1.0}\ (3d\sigma_u)^{1.0}\ (3d\pi_u)^{3.5}\ (3d\pi_g)^{2.4}\ (3d\delta_g)^{3.6}\ (3d\delta_u)^{2.3}\ (4s\sigma_g)^{1.0}\ (4s\sigma_u)^{0.1})$. The Fe-Fe bond, is then, constituted to 1.65 of the total bond order which contains 27.3% σ, 33.3% π, and 39.4% δ contributions. This bond is a weaker bond when compared with Fe_2 and

has longer Fe-Fe distance. Compared with the experimental IP_1 of 6.30±0.01 eV, our best calculation predicted the IP_1 of 5.1 eV while Tomonari et al. predicted 4.79 eV. Thus, our calculations have the best prediction for IP_1 which supports our Fe_2 and Fe_2^+ electronic structures. For the Fe_2^- molecule, the electronic state is $^8\Delta_g$ state. The R_e and the ω_e obtained from our best calculations are 4.03 Bohr and 278.2 cm^{-1} respectively while the experimental R_e and ω_e are 3.89-4.04 Bohr and 250±20 cm^{-1}, respectively [4]. The occupation numbers of the natural orbitals revealed the electronic configuration of $((3d\sigma_g)^{1.7}\ (3d\sigma_u)^{1.2}\ (3d\pi_u)^{3.3}\ (3d\pi_g)^{2.5}\ (3d\delta_g)^{3.7}\ (3d\delta_u)^{2.4}\ (4s\sigma_g)^{1.0}\ (4s\sigma_u)^{1.0})$. The Fe-Fe bond in Fe_2^- has the total bond order of 1.30 which contributed by 19.2% σ, 30.8% π, and 50.0% δ bonds, the relatively weaker bond compared to Fe_2 but with a slightly longer R_e. From the Fe_2^- and Fe_2 energy, the EA was computed and the value of 0.316 eV was obtained while experimentally the EA of 0.902±0.008 eV [4] was reported. Interestingly, Tomonari et al. [8] also suggested the EA of 0.46 eV which is closer to our prediction than that of the experiment. Possibly, the basis set for Fe_2^- is still not large enough and better EA could be obtained if larger basis set is employed. For the Fe_2^{++} molecule, the 4 electronic states were investigated, *i.e.* $^9\Delta_u$, $^9\Pi_g$, $^7\Delta_g$ and $^7\Pi_u$. For each electronic state, only the 5432 basis is used. From our calculation, the $^9\Pi_g$ state appears to be the electronic ground state of the Fe_2^{++} molecule with the energy of roughly 30 kcal/mol below the next lowest state. The occupation numbers of the natural orbitals revealed the electronic configuration of $((3d\sigma_g)^{1.0}\ (3d\sigma_u)^{1.0}\ (3d\pi_u)^{2.5}\ (3d\pi_g)^{2.4}\ (3d\delta_g)^{3.5}\ (3d\delta_u)^{2.4}\ (4s\sigma_g)^{1.0}\ (4s\sigma_u)^{0.0})$ for the $^9\Pi_g$ Fe_2^{++}. The bonding in this state has 1.10 bond order which comprises of 45.5% σ, 4.5% π and 50.0% δ bond. The calculated R_e and ω_e are 5.29 Bohr and 176.5 cm^{-1}. The computed IP_2 of 15.9 eV was reported. Thus, the much stronger 2nd ionization was observed. The electronic ground states, R_e, ω_e , and

the natural occupations of Fe_2, Fe_2^+, Fe_2^-, and Fe_2^{++} were summarized in Table **27**. The calculated and experimental IP_1, the IP_2, and the EA of these compounds were given in Table **28**.

Table **27**: The natural orbitals, R_e, and $omega_e$ of Fe_2, Fe_2^+, Fe_2^-, and Fe_2^{++}.

$3d\sigma_g$	$3d\sigma_u$	$3d\pi_u$	$3d\pi_g$	$3d\delta_g$	$3d\delta_u$	$4s\sigma_g$	$4s\sigma_u$	R_e	ω_e
The Fe_2 molecule, $^7\Delta_u$ state (R_e = 3.82±0.04 Bohr, ω_e = 299.6 cm^{-1})									
1.7	1.2	3.5	2.4	3.7	2.3	1.0	0.0	3.96	453.6
The Fe_2^+ molecule, $^8\Delta_u$ state									
1.0	1.0	3.5	2.4	3.6	2.3	1.0	0.1	4.49	159.6
The Fe_2^- molecule, $^8\Delta_g$ state (R_e = 3.89-4.04Bohr, ω_e = 250±20 cm^{-1})									
1.7	1.2	3.3	2.5	3.7	2.4	1.0	1.0	4.03	278.2
The Fe_2^{++} molecule, $^9\Pi_g$ state									
1.0	1.0	2.5	2.4	3.5	2.4	1.0	0.0	5.16	176.4

Table **28**: The IP_1, IP_2, and EA of Fe_2 molecule.

	IP_1 (eV)	IP_2 (eV)	EA (eV)
CI	4.97	15.1	0.288
CI+Q	5.09	15.9	0.316
Tomonari and Tatewaki	4.79	-	0.450
Experimental	6.30±0.01	-	0.902±0.008

REFERENCES

[1] Rohlfing, E.A., Cox, D.M., Kaldor, A., and Johnson, K.H. **Photoionization spectra and electronic structure of small iron clusters.** *J. Chem. Phys.* 81(9), **1984**: 3846.

[2] Montano, P.A., and Shenoy, G.K. **EXAFS study of iron monomers and dimers isolated in solid argon.** *Solid State Comm.* 35, **1980**: 53.

[3] Purdum, H., Montano, P.A., Shenoy, G.K., and Morrison, T. **Extended-x-ray-absorption-fine-structure study of small Fe molecules isolated in solid neon.** *Phys. Rev. B* 25, **1982**: 4412.

[4] Leopold, D.G., and Lineberger, W.C. **A study of the low-lying electronic states of Fe_2 and Co_2 by negative ion photoelectron spectroscopy.** *J. Chem. Phys.* 85(1), **1986**: 51.

[5] Harris, J., and Jones, R.O. **Density functional theory and molecular bonding. III. Iron-series dimers.** *J. Chem. Phys.* 70(02), **1979**: 830.

[6] Guenzburger, D., and Saitovitch, E.M.B. **Fe dimers: A theoretical study of the hyperfine interactions.** *Phys. Rev. B* 24, **1981**: 2368.

[7] Shim, I., and Gingerich, K.A. *Ab initio* **HF-CI calculations of the electronic "band structure" in the Fe_2 molecule.** *J. Chem. Phys.* 77(5), **1982**: 2490.

[8] Tomonari, M., and Tatewaki, H. **The ground, excited, and negatively ionized states of Fe_2.** *J. Chem. Phys.* 88(3), **1988**: 1828.

[9] Nagarathna, H.M., Montano, P.A., and Naik, V.M. **Matrix Tsolation Study of FeCr Molecules and SCF-$X\alpha$-Scattered Wave Molecular Orbital**

Calculation on Fe_2 and FeCr Diatomics. *J. Am. Chem. Soc.* 105, **1983**: 2938.

[10] Levine, I.N. **Quantum Chemistry.** Fourth Edition. New York: Prentice-Hall International, 1991.

[11] Helgaker, T., Jørgensen, P., Olsen, J. **MOLECULAR ELECTRONIC-STRUCTURE THEORY.** The first edition. Chicheter: John wiley & sons, 2000.

[12] Szabo, A., Ostlund, N.S. **MODERN QUANTUM CHEMISTRY Introduction to Advanced Electronic Structure Theory.** First Edition, Revised. New York: Dover publications, 1996.

[13] Almlöf, J., and Taylor, P.R. **General contraction of Gaussian basis sets. I. Atomic natural orbitals for first- and second-row atoms.** *J. Chem. Phys.* 86, **1987**: 4070.

[14] Pierloot, K., Dumez, B., Widmark, P.-O., and Roos, R.O. **Density matrix averaged atomic natural orbital (ANO) basis sets for correlated molecular wave functions. IV. Medium size basis sets for the atoms H-Kr.** *Theor. Chim. Acta.* 90, **1995**: 87.

[15] COLUMBUS, An *ab initio* Electronic Structure Program, Release 5.3, **1997**, written by Lischka, H., Shepard, R., Shavitt, I., Brown, F.B., Pitzer, R.M., Ahlrichs, R., Böhm, H.-J., Chang, A.H.H., Comeau, D.C., Gdanitz, R., Dachsel, H., Dallos, M., Erhard, C., Ernzerhof, M., Gawboy, G., Höchtl, P., Irle, S., Kedziora, G., Kovar, T., Müller, T., Parasuk, V., Pepper, M., Scharf, P., Schiffer, H., Schindler, M., Schüler, M., Stahlberg, E., Szalay, P.G., and Zhao, J.G.

[16] Shepard, R., Shavitt, I., Pitzer, R.M., Comeau, D.C., Pepper, M., Lischka, H., Szalay, P.G., Ahlrichs, R., Brown, F.B., and Zhao, J.-G. **A Progress Report on the Status of the COLUMBUS MRCI Program System.** *Int. J. Quantum Chem.* S22, **1988**: 149.

[17] Harris, D.C., Bertolucci, M.D. **SYMMETRY AND SPECTROSCOPY An Introduction to Vibrational and Electronic Spectroscopy.** The first edition. New York: Dover publications, 1989.

[18] Tatewaki, H., Tomonari, M., and Nakamura T. **The band structure of small iron clusters from Fe_1 to Fe_6.** *J. Chem. Phys.* 88, **1988**: 6419.

[19] Dyson, W., and Montano, P.A. **NEAREST NEIGHBOR EFFECT ON THE ISOMER SHIFT OF ^{57}Fe IN SMALL METAL CLUSTER.** *Solid State Comm.* 33, **1980**: 191.

[20] McNab, T.K., Micklitz, H., and Narrett, P.H. **Mössbauer Studies on ^{57}Fe Atoms in Rare-Gas Matrices between 1.45 and 20.5 K.** *Phys. Rev. B* 4, **1981**: 3787.

VITA

Mr. Viwat Vchirawongkwin was born on April 22, 1976 in Bangkok, Thailand. He graduated with a Bachelor Degree of Science in Chemistry from Chulalongkorn University in 1988. During the same year, he was admitted into Master's Degree Program in physical chemistry at Chulalongkorn University. He finishes his Master's Degree in the year 2001.